Energy Conversion and Management 351 (2026) 120973

Contents lists available at ScienceDirect

Energy Conversion and Management

journal homepage: www.elsevier.com/locate/enconman

Research Paper

Standardized techno-economic assessment of synthetic natural gas and synthetic hydrogen natural gas production for the transport sector and gas grid

Nathanael Heimann [a,*], Francisco Moser [a], Moritz Raab [a], Jens Hüttenrauch [b], Ralph-Uwe Dietrich [a]

[a] German Aerospace Center e.V. (DLR), Institute of Engineering Thermodynamics, Pfaffenwaldring 38-40, 70569 Stuttgart, Germany
[b] DBI Gas- Und Umwelttechnik GmbH, Karl-Heine-Straße 109/111, D-04229 Leipzig, Germany

ARTICLE INFO

Keywords:
CNG
Synfuel
HSNG
SNG
PtG

ABSTRACT

As CO_2-emission hit new records, immediate emission reductions have to be achieved, especially in the transport and industrial sector an in domestic heat. As important backbone of the industrial and private sector, the existing natural gas grid is capable of storing and transporting large amounts of energy. Admixing synthetic natural gas to the gas grid could have an immediate impact on CO_2-safings. Furthermore, admixing up to 30 % renewable H_2 to the gas grid could improve resilience, lower costs, compared to synthetic natural gas, and could have positive impacts on the use in the transport sector.

Based on rigorous process simulations in Aspen Plus® V14 a techno-economic analysis for two production processes: high temperature TREMP™ and low temperature isothermal, has been carried out. The product quality has been set to the overlap of the requirements of the gas grid and the transport sector. Furthermore, three different higher hydrogen concentrations have been assessed. The TREMP™ process has a power-to-fuel-efficiency of about 57 % compared to 55 % for the isothermal process, resulting in net production costs in 2018 of 185 $€_{2018}$ MWh_{LHV}^{-1} for TREMP™ versus 189 $€_{2018}$ MWh_{LHV}^{-1} for isothermal. An increase from 2 % to 30 % mol H_2 reduces the NPC by about 2.6 % for TREMP™ and 2.7 % for the isothermal process in comparison to synthetic natural gas. Technical constraints and costs within the gas grid suggest a sweet spot of hydrogen admixture of up to 20 % vol. H_2.

1. Introduction

According to the Paris agreement greenhouse gas (GHG) emissions should be cut to halve by 2030 compared to pre-industrial times [1]. Yet, global GHG emissions hit an new record in 2024 with 37.8 GT CO_2 [2]. Especially for transport, industrial combustion processes and buildings, higher efforts have to be undertaken as their worldwide combined GHG emissions account for about 45 % of total emissions [3].

Natural gas as the"largest contributor to global carbon emissions growth", IEA [2], could be produced renewably. If carbon dioxide is the carbon source, methanol and methane can be produced more efficiently than other renewable synthetic fuels (synfuel) [4]. Since, the production of synthetic natural gas (SNG) is a well-established process, available at commercial scale [5], ramping up its renewable production and use might have immediate positive effects on GHG emissions. As the existing natural gas grid is one of the most important backbones of the industrial and private sector and is capable of storing large amounts of energy, its use for SNG or renewable methane-hydrogen-blends (HSNG) is probably more sensible than partially tearing it down and replacing it by an H_2-grid or paying for a dual structure, as currently planned in Germany, for example [6].

Direct electrification of the transport sector might be feasible in parts, still for hard-to abate sectors renewable fuels might be important. Natural gas could be used in an internal combustion engine leading to up to 20 % lower CO_2 emissions than gasoline and diesel [7]. If produced renewable, CO_2 emissions could decrease even further. Additionally, natural gas combustion emits less nitrogen oxides (NOx) and $PM_{2.5}$ than its diesel counterpart [8]. The amount of CNG and liquefied natural gas (LNG) trucks has already increased, for instance on the German market [9]. This was supported by a toll exemption between 2021 and 2022, by subsidies for fleet replacement and by increasing the number of CNG/

* Corresponding author.
E-mail address: nathanael.heimann@dlr.de (N. Heimann).

https://doi.org/10.1016/j.enconman.2025.120973
Received 24 March 2025; Received in revised form 9 December 2025; Accepted 18 December 2025
Available online 16 January 2026

Nomenclature

ACC	Annual Capital Costs[€ a^{-1}]
CEPCI	Chemical Engineering Plant Cost Index[-]
$E_{By-product}$	Exergy of by-products[MW_{ex}]
E_{ci}	Equipment cost of function i[€]
E_{CO_2}	Exergy of carbon dioxide flowing into the process[MW_{ex}]
$E_{Electricity,generated}$	Electricity generated by the process[MW_{ex}]
$E_{Electricity,Plant}$	Electricity needed for the process excluding H_2 production and CO_2 purification[MW_{ex}]
E_{H_2}	Exergy of hydrogen flowing into the process[MW_{ex}]
$E_{Heat,Synfuel}$	Exergy of heat of synfuel[MW_{ex}]
$E_{Net,Heat}$	Exergy of heat (net resources spent to generate the product)[MW_{ex}]
FCI	Fixed Capital Investment[€]
$F_{eco,I,j}$	Economic factor j for equipment i[-]
f_i	Equipment cost of function i[€]
$F_{material,i}$	Material factor of the equipment i[-]
$F_{pressure,i}$	Pressure factor of the equipment i[-]
IR	Interest Rate[-]
K_{eq}	Equilibrium constant[K]
K_{mix}	Equilibrium constant of mixing[K]
NPC	Net production Costs[€]
$OPEX_{dir}$	Direct Operational Expenditures[€]
$OPEX_{ind}$	Indirect Operational Expenditures[€]
$S_{i,j}$	Entry variable j of the cost function[-]
t_{labor}	Labor hours[h]
T_{ref}	Reference Temperature[K]
y	Plant Operating Time[a]
$\varepsilon_{Process-to-X}$	Process-to-X exergy efficiency[-]
ε_{PtF}	Power-to-fuel exergy efficiency[-]
η_{HtF}	Hydrogen-to-fuel efficiency[-]
η_{HtF}	Compressed Natural Gas[-]
η_{PtF}	Power-to-fuel efficiency[-]
ΔH_R^o	Enthalpy of Reaction[-]
j	Index 1 CO-methanation; Index 2: RWGS
n	OH, mix, C, H, CO, H_2, CH_4, H_2O
AEL	Alkaline Water Electrolysis
CNG	Compressed Natural Gas
GHG	Greenhouse Gas
GHSV	Gas Hourly Space Velocity
HSNG	Hydrogen Synthetic Natural Gas
iso	Low temperature isothermal process
LHV	Lover heating value of synfuel
LNG	Liquefied Natural Gas
OPEX	Operational Expenditures
PEM	Proton Exchange Membrane
PPA	Power Purchase Agreement
SOEC	Solid Oxide Electrolyzer Cell
Synfuel	Synthetic fuel
TREMP	TREMP™: Topsøe's Recycle Energy-Efficient Methanation Process
TRL	Technology Readiness Level

LNG filling stations in Germany [7]. Moreover, LNG is a viable ship fuel [10].

By producing renewable HSNG instead of SNG, synthesis losses could be reduced. Up to 30 % hydrogen in natural gas grid seem to be feasible without mayor changes [11]. Adding hydrogen to methane for transport applications could have positive effects as well. Dimopoulos et al. [12], for instance, analyzed that having 15 vol% H_2 in natural gas could lead to an increase of 3 % engine efficiency while engine-out NO_x emissions could be lowered by 45 % with no change in CO-emissions. Hydrocarbons emissions increased by 7 %. However, methane slip can be oxidized by about 80 % to 98 % by catalysts [13].

Besides technical considerations, the production cost of synfuels and their competitiveness to other alternatives are key aspects for their implementation in the market. Still, comparison of production costs is difficult, since publications are carried out under a variety of assumptions as outlined for instance by Heimann et al. [14]. Here are some more examples for SNG: Gorre et al. [15] calculated methane costs as low as 16 € MWh_{LHV}^{-1}. This is based on assumed low (future) electricity costs or future governmental funding. Comparably high costs of 410 to 590 $€_{2020}$ MWh_{LHV}^{-1} as in Vega Puga et. al. [16], might be due to their small plant size, their equipment costs functions and their relatively high surcharge factors. Their statement, that the CO_2-price is neglectable, is based on their assumptions, that the CO_2-extraction has no costs and their high share of capital expenses in the production costs. In some publications, neither the year of the analysis [17] nor the plant lifetime [18] is specified, hence no comparison of production costs is feasible. The same is true, if the product purity is not given [15,19] or differs between publications. Further influences such as full-load-hours, plant capacity and country/location have also considerable influence on the comparability of results. A selection of recent publications on power to methane is summarized in the supplementary information (SI) in Table S1.

In this work a techno-economic analysis for SNG meeting quality standard of both, the gas grid (Germany) and the transport sector is carried out for a high-temperature process, Topsøe's Recycle Energy-Efficient Methanation Process, TREMP™ (TREMP), and a low-temperature isothermal process (iso). Results are directly compared with the production of renewable methanol, published by Rahmat et. al. [20]. In addition, the production of various HSNG mixtures will be evaluated and technical and economic options for a smooth transition of the gas grid, including HSNG mixtures, will be presented.

2. Methods

In this chapter the product gas composition and educts are defined, as well technical, economical parameters and used methodologies. The main basic assumptions are used as in Heimann et al. [14].

2.1. Definition of product gas composition according to standards

For comparable results, the purity of the SNG is defined. Two standards have been considered:

- DIN EN 16723–2:2017–10 "Natural gas and biomethane for use in transport and biomethane for injection in the natural gas network – Part 2: Automotive fuels specification" [21]
- DVGW G260 "Gas quality" [22]

for the overlap of both standards, the product can be used in internal combustion engines as well as it can be injected into the gas grid. The composition of the SNG was defined by maximizing the hydrogen content to the 2 % mol limit of the standard DIN EN 16723–2:2017–10 due to its high gravimetric energy content, lower CO_2 need in the production and advantages in the combustion. For the sake of simplicity, the presence of CO in the product is neglected being less than 0.05 % mol for the high-temperature methanation process, TREMP. Furthermore CO is not considered in the kinetic of Koschany et al., which is used in the isothermal process [23]. The CO_2 content was minimized to 0.3 % vol., to reach lower density limit of the standards.

Additional to SNG, the production of three HSNG blends is analyzed.

Since the standard DIN EN 16723–2:2017–10 states that hydrogen concentration of up to 10 % vol. might be used for special gas motors, a HSNG-10 (10 % vol. H_2) mixture was defined. Furthermore, HSNG-20 (20 % vol. H_2) and HSNG-30 (30 % vol. H_2) mixtures were incorporated. Since there are no standard for HSNG-mixtures, the limits have been defined by the authors. The resulting composition of SNG and HSNG is presented in Table 1.

2.2. Electricity

The energy supply costs are the most relevant input variable regarding the cost of a PtX–product [26]. In this study, the following electricity sources have been selected in order to be comparable with results of Rahmat et al. [20]:

- *Case 1* – Grid electricity for 2018 and estimations for 2030 and 2045 as in [14,20].
- *Case 2* – Renewable German grid electricity as also implemented in [20], with prices from the German day-ahead market using 2020 values and, guarantees of origin.
- *Case 3* – Local production as also implemented in [20], with a combination of a PV farm, wind turbines, storages and curtailment for a constant H_2-production using the methodology as presented in Raab et al. [27].

2.2.1. Renewable grid electricity 2020 (Case 2)

For the estimation of the renewable grid electricity price, the prices are divided into the different components such as taxes, levies, distribution-, electricity procurement price and others [28]. The year 2020 has been selected as a year with exceptional low electricity prices and can be seen as a best case. Green electricity is ensured by guarantees of origin, or power purchase agreement (PPA). Since these contracts are usually confidential and differ a lot depending on the contractors, a published surcharge for guarantees of origin has been used [29]. For the scope of this investigation, the German electricity market is utilized as a reference to estimate the electricity cost. The price components are divided in three main categories (Measurement and billing, Network charges, Taxes and levies) following the analysis used by Grave et al. [28]. Electricity procurement prices are defined as the purchase costs of electricity, also encompassing the margins of the suppliers. To estimate these prices, the average of the day-ahead-price for the year 2020 [30] was used. Network charges are defined as the charges associated with the transmission and distribution of electricity by the system operators. Other state-regulated components are costs which are defined by energy policy instruments or state revenue requirements. This component includes taxes and levies but also costs associated with meeting specified quotas. For the calculation of levies and taxes the yearly electrical demand plays a significant role in the specific cost of several of the levies or taxes. Therefore, the electricity cost was calculated for an electrical demand of 2,400 $GWh_{el}\ a^{-1}$, resulting from a full load operation of 8,000 $h\ a^{-1}$ and an assumed power demand of 300 MW_{el}. The resulting electricity prices are listed in Table 2. More detailed values are shown in the

Table 2
Input values of evaluated cost cases.

Year	Case		Electricity price	H_2 cost	CO_2 cost	Reference
			€$_{2018}$ MWh_{el}^{-1}	€$_{2018}$ kg^{-1}	€$_{2018}$ t^{-1}	
2018	Case 1	min	55.72	4.74	68.95	[14]
		max	89.60	6.43	73.13	[14]
2020	*Case 2:* 100 % RE-grid		42.15	3.66	71.63[b]	
	Case 3: 100 % RE-Stötten		42.15[a]	10.51	71.63[b]	
	Case 3: 100 % RE-Friesoythe		42.15[a]	11.44	71.63[b]	
2030	Case 1	min	66.13	3.96	82.19	[14]
		max	99.43	5.51	87.52	[14]
2045	Case 1	min	40.51	2.34	89.61	[14]
		max	63.00	3.33	93.42	[14]

a) Assumed for electrical demand of the synthesis plant, not for electrolyzer or CO_2-extraction used.
b) Linearly interpolated from 2018 to 2030.

Table 1
Composition and properties of selected synthetic fuels and requirements of CNG according to DIN EN 16723–2:2017–10 [21] and DVGW G260 [22].

Properties		DIN EN 16723–2 (Gas 2H)		DVGW G260		SNG	HSNG-10	HSNG-20	HSNG-30
		min.	max.	min.	max.				
Methane content	% vol.	–	–	–	–	97.7	89.7	79.8	69.8
CO_2 content	% vol.	–	5[c]	–	2.5	0.3	0.3	0.2	0.2
Oxygen content	% vol.	–	1	–	3[g] / 0.001[h]	0	0	0	0
Hydrogen content	% vol.	–	2	–	–	2	10	20	30
Mass LHV	$MJ\ kg^{-1}$					49.8	50.6	51.8	53.2
Mass LHV	$kWh\ kg^{-1}$					13.8	14.0	14.4	14.8
Density absolute at 15 °C	$kg\ m^{-3}$	–	–	0.67[f]	0.92[f]	0.67 [k]	0.62[k]	0.56[k]	0.50[k]
Methane number [a]	–	70[b]	–	–	–	96[k]	83[k]	71[k]	61[k]
Water dew point for p = 20 bar	°C	–	−30 [d]	–	–	−30	−30	−30	−30
Water content	$mg\ m^{-3}$	–	–	–	200 [i] / 50 [j]	–	–	–	–
Pressure	bar	–	20 [e]	–	–	20	20	20	20
Wobbe-Index (higher)	$MJ\ m^{-3}$	45.7	54.7	46.5[f]	53.7[f]	53.0[k]	51.9[k]	50.6[k]	49.3[k]

a) Calculated using Wärtsilä Corporation's calculator [24].
b) According to the standard, only a small portion of the natural gas can have a methane number lower than 70.
c) 5 % mol is max. $CO_2 + N_2 + O_2$ content.
d) Highest requirement in the standard selected.
e) Definition of CNG implies a pressure of 20,000 kPa.
f) Recalculated using 15 °C as reference temperature.
g) Maximal Operating Pressure (MOP) ≤ 16 bar.
h) Maximal Operating Pressure (MOP) < 10 bar.
i) Maximal Operating Pressure (MOP) ≥ 10 bar.
j) Selected to ensure the minimum gas density while maximizing the H_2 content. For the sake of simplicity, the sum of CO_2 and CO will be used for this specific measurement.
k) Values have been calculated using ISO 6976 with [25].

SI in Table S2.

2.2.2. Local renewable stand-alone electricity 2020 (Case 3)

For *Case 3*, the locations of Friesoythe (N53.03, E7.86) and Stötten (N48.65, E9.86) are selected due to their attractive renewable energy potential in Germany. Weather data from the German Weather Service Climate Data Center [31] are used as input to determine the production potential of renewable energy. The costs for electricity and hydrogen from a PV farm and wind turbines are retrieved with the tool of Raab et al. [27]. The costs for a utility scale PV farm and wind turbines are taken from IRENA [32]. This way, an isolated location without grid connections can be assessed. Electricity costs for all three cases are presented in Table 2.

2.3. Hydrogen supply costs

Based on the three electricity cases, there are three hydrogen cases. The hydrogen source from *Case 1* is based on equal production shares from proton exchange membrane electrolyzer (PEM), alkaline water electrolyzer (AEL) and solid oxide electrolyzer cell (SOEC) as a generic assumption and the underlying electricity price is the same as in the electricity *Case 1* as in [14]. Underlying electrolyzer efficiencies are attached in the SI in Table S3. For the renewable energy cases (*Case 2* and *Case 3)* the cheapest electrolyzer technology, AEL, is selected. Since in *Case 3* the renewable energy is fluctuating but the subsequent methane process runs stead-state, hydrogen is produced and is either feed to the synthesis plant or to a compressed hydrogen storage tank. If there is less electricity available than needed, hydrogen from the tank is used. Curtailment of the renewable energy is included, if the storage tank is filled and electricity is still generated. For the size of the electrolyzer and storage tank an optimization on lowest levelized cost of hydrogen with perfect forecast has been developed and presented in Raab et al. [27]. The technical and economic input data, i.e., efficiency and investment costs, for the years 2018 and 2030 are taken from [14] and linearly interpolated for the year 2020 in *Case 2* and *3*. Resulting values are presented in Table 2.

2.4. Carbon dioxide supply costs

CO_2 costs for *Case 1* are taken from [14] and are listed in Table 2. Since the selection of a CO_2-source depends on local availability and regulations, a "generic CO_2-source" has been selected with average CO_2-costs. It represents a mixture of direct air capture (0 % - 10 %), and ethanolamine-wash-extraction of the point sources cement plant (70 % – 45 %), gas and steam power plant (15 % – 25 %) and waste incineration plant (15 % – 20 %). The exact shares by year are reported in the SI in Table S4. For the year 2020, the cost calculation methodology form [14] is used with interpolated shares of CO_2-sources. The renewable grid electricity costs for the year 2020 are used the calculation of the CO_2 costs for *Case 2* and *Case 3*.

2.5. Kinetic and thermodynamic models

The process models have been simulated in Aspen Plus® V14 with the property method of Soave-Redlich- Kwong to account for real gas behavior. In the following sections, the kinetic models are described.

2.5.1. Reaction kinetic models

The methanation process can be described by three chemical equations: The CO methanation eq. (1), the reverse water–gas shift eq. (2), and the CO_2 methanation eq. (3). The latter is assumed as a linear combination of eq. (1) and eq. (2) [5].

$$CO + 3H_2 \leftrightarrow CH_4 + H_2O \Delta H_R^o = -206 \frac{kJ}{mol} \quad (1)$$

$$CO_2 + H_2 \leftrightarrow CO + H_2O \Delta H_R^o = +41 \frac{kJ}{mol} \quad (2)$$

$$CO_2 + 4H_2 \leftrightarrow CH_4 + 2H_2O\ \Delta H_R^o = -164 \frac{kJ}{mol} \quad (3)$$

Rönsch et al. [5] present an overview of more than ten different established methanation concepts, categorizing them by their maximum temperature and development state. In their publication, the adiabatic fixed bed reactors have the maximal technology readiness level (TRL) TRL9. The other reactor types with lower TRL are: fixed bed reactors and fluidized bed reactors with TRL7, i.e., system prototype demonstration in an operational environment.

In this work, an adiabatic fixed bed reactor process and a cooled multi-tubular fixed bed reactor process are investigated. For the former, TREMP is selected since it is already available on a commercial level [5]. Furthermore, it is optimized for the production of overheated steam, which can be used to generate electricity, making it highly efficient. High energetic efficiency promises lower production cost, what shall be confirmed and quantified within this study. The isothermal process, on the other hand, focuses on keeping the temperatures in the reactor low, thus, decreasing the danger of catalyst sintering. Since TREMP and the isothermal process run with different catalysts, temperatures and pressures, they are simulated with different kinetics.

2.5.1.1. TREMP. TREMP is simulated using the CO-methanation kinetics of Klose et al. [33] for a catalyst with 18 % mass nickel, as a conservative approach for the MCR-2X catalyst (22 % mass nickel) used in commercial applications [34]. Since the kinetics is developed for a pressure range of 20 to 30 bar, it should be applicable within the operation pressure of TREMP at about 27 bar [34]. To allow for the simulation of the CO_2 methanation, CO methanation kinetic is complemented with the RWGS kinetics of Zhang et al. [35], updated by Rönsch et al. [36]. The chosen reaction equations are shown in eq. (4) to (7).

$$r_{Meth,18\,\%Ni} = \frac{k_{1,\,Klose} K_C K_H^2 \bullet p_{CH_4} \bullet p_{H_2O} \bullet p_{CO}^{-0.5} \bullet p_{H_2}^{-2} \left(\frac{1}{K_{Meth}}\right)}{\left(1 + K_C p_{CO}^{0.5} + K_H p_{H_2}^{0.5}\right)^3} - \frac{k_{1,\,Klose} K_C K_H^2 \bullet p_{CO}^{0.5} \bullet p_{H_2}}{\left(1 + K_C p_{CO}^{0.5} + K_H p_{H_2}^{0.5}\right)^3} \quad (4)$$

$$r_{WGS} = \frac{\frac{k_2}{p_{H_2}} \left(p_{CO} \bullet p_{H_2O} - \frac{p_{H_2} \bullet p_{CO_2}}{K_{WGS}}\right)}{\left(1 + K_{CO} p_{CO} + K_{H_2} p_{H_2} + K_{CH_4} p_{CH_4} + \frac{K_{H_2O} p_{H_2O}}{p_{H_2}}\right)^2} \quad (5)$$

$$k_j = k_j^0 \exp\left(-\frac{E_n}{RT_G}\right) \quad (6)$$

$$K_n = K_n^0 \exp\left(-\frac{\Delta H_n}{RT_G}\right) \quad (7)$$

The index j equals 1 for CO-methanation and j = 2 for the reverse water–gas shift reaction. The index n stands for the adsorbed species C, H, CO, H_2, CH_4, and H_2O. The temperature-dependent constants K_{WGS} and K_{Meth} have been calculated according to Elnashaie et al. [37]. Underlying parameters are listed in the SI in Table S5 and in Figures S1 and S2 of the SI, the validation of the kinetics for the Aspen Plus ® simulation is included.

2.5.1.2. Isotherm process. The isothermal process is simulated with the kinetics of Koschany et al. [23]. It can be used for a catalyst with 35 % mass nickel with an operating temperature between 250 and 310 °C and a pressure between 3 and 9 bar. In his dissertation, Koschany [38]

evaluated different kinetic approaches according to his findings, the Langmuir-Hinshelwood-Hougen-Watson model delivered the most fitting results. Thus, it is implemented in the simulation, as for equations (8) to (10).

$$r_{LHHW,\ Koschany} = \frac{k_{\text{Koschany}} \bullet p_{CO_2}^{0.5} \bullet p_{H_2}^{0.5} \left(1 - \frac{p_{H_2O}^2 p_{CH_4}}{p_{CO_2} p_{H_2}^4 K_{eq}}\right)}{\left(1 + K_{OH} \frac{p_{H_2O}}{p_{H_2}^{0.5}} + K_{H_2} p_{H_2}^{0.5} + K_{mix} p_{CO_2}^{0.5}\right)^2} \quad (8)$$

$$k_{Koschany} = k_0 exp\left(\frac{E_a}{R}\left(\frac{1}{T_{ref}} - \frac{1}{T_G}\right)\right) \quad (9)$$

$$K_n = K_n^0 exp\left(-\frac{\Delta H_n}{RT_G}\left(\frac{1}{T_{ref}} - \frac{1}{T_G}\right)\right) \quad (10)$$

Here, T_{ref}T$_{\text{ref}}$ is the reference temperature. Index n stands for the adsorbed species OH, H_2 and for the mixture. The equilibrium constant, K_{eq},K$_{\text{eq}}$ is calculated using equation (11) from Aparicio [39].

$$K_{eq} = 137 \cdot T^{-3.998} exp\left(\frac{158.7\,kJ/mol}{RT}\right) \quad (11)$$

The equilibrium constant of mixing, K$_{\text{mix}}$K$_{\text{mix}}$, is calculated using (12) and the excess Gibbs free energy of mixing, A_{mix}A$_{\text{mix}}$.

$$K_n^0 = exp\left(-\frac{A_n}{R}\left(\frac{1}{T_{ref}} - \frac{1}{T}\right)\right) \quad (12)$$

The kinetic parameters are attached in the SI in Table S6. Simulation results have been shared with partners from industry and research within the project BEniVer [40] and resemble best knowledge of all the partners.

2.6. Simulation Description

Methanation is an exothermic process with high product concentration at low temperatures but high reaction rates at high temperatures. Therefore, temperature control is vital. If the temperature rises too high, sintering of the catalyst and deactivation can take place, as described by Champon et al. [41]. Too low temperatures require large reactors for the low reaction rate. A technical and economical optimum has to be selected. In this work, two approaches are compared. No by-product formation is assumed as the catalysts are considered very selective. Furthermore, no technical heat-losses are assumed, to be comparable with the results of Rahmat et al. [20].

2.6.1. Adapted TREMP process

To make use of the waste-heat, Topsøe presented the TREMP™-process [42]. It is a high-temperature adiabatic methanation process with a nickel-based catalyst [43]. Consisting of three to four adiabatic reactors, each one is running at lower temperatures as the previous one and has inter-stage cooling. It is capable of producing synthetic natural gas compatible with pipeline specifications and the process and catalysts are commercially available [44]. As the first reactor runs at temperatures of about 700 °C, heat can be recovered to produce steam for electricity generation. For temperature control in the first reactor, educts are diluted with products by a recycle. The catalyst (MCR-2X) can withstand temperatures up to 800 °C [42]. Its lifetime is assumed to be 8,000 h as in Meylan et al. [45].

In this work, the TREMP™ process is altered by adding a fifth reactor (polishing reactor), to ensure a maximum hydrogen content of 2 % in the SNG, and by an additional water removal step at the end to keep the water content under the dew point of −30 °C. Fig. 1 shows the flow diagram for the adapted TREMP process including the necessary changes.

The inlet pressure is set to 27.2 bar according to experimental values of Harms et al. [34] and pressure drops are calculated the Ergun-equation in Aspen Plus®. The temperature of the hydrogen and CO_2 streams before entering the mixer (M1) are specified to reach a reactor inlet temperature of 250 °C, which is in the range of the process set-up [42]. The amount of recycled gas for R1 is set to not exceed an outlet-temperature of 700 °C. High temperature steam is generated in HX3. Water removal at the intercooling in between the reactors at flash (F1, F2) moves the equilibrium concentration to the product-side. The inlet temperatures of the reactors R2, R3 and R4 are adjusted to achieve a maximum conversion rate and R5 to achieve the specified output concentration. The gas hourly space velocity (GHSV) of each stage is set to reach equilibrium concentration close to the reactor end with 10 % over-dimensioning to account for potential catalyst deactivation as in real applications. The length of each reactor is set to 2 m and the diameter is adapted according to the GHSV value. In a real plant, the sizes would also be adapted according to supplier specifications. The catalyst has a bed voidage of 0.3 and a particle density of 500 kg m^{-3}. The reaction rate in the first reactors is very high, as also in the experiments of Harms et al. [34]. Therefore, the first reactors has been limited to a GHSV of 8,000 h^{-1} even though reaction to equilibrium occurs in the first decimeters of the reactor. The reactors have been simulated in Aspen Plus® with 'Rplug' without tubes. Heat integration has been done by a PINCH-analysis. The chosen GHSV-values are attached in the SI in Table S8 for different product hydrogen concentrations. In Table S16-S19, the temperatures and concentrations of the process streams are attached, as well as the dimensions of each reactor.

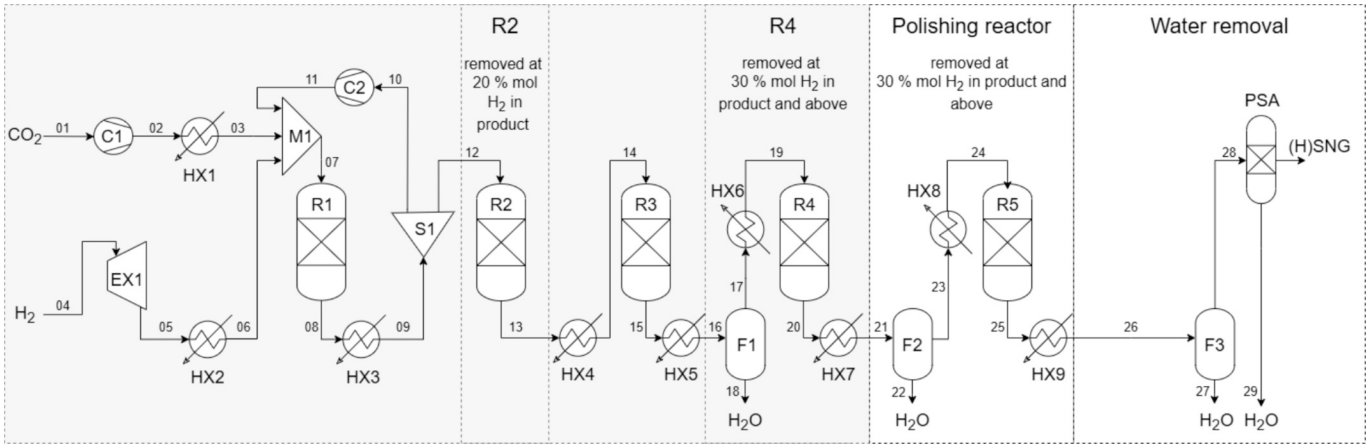

Fig. 1. Flow diagram of adapted TREMP process for SNG and HSNG.

2.6.2. Isothermal Process

The configuration of the isothermal process is presented in Fig. 2.

To run the reactors below 285 °C the hydrogen is feed by 60 % to the first and 40 % to the second reactor, decreasing the reaction rate. Additionally, the feed is diluted with steam to avoid carbon deposition conditions and further decrease the rate of reaction. Furthermore, the catalyst is mixed with an inert component of SiC particles with a mass ratio of $m_{SiC}\ m_{Kat}^{-1} = 9$, as in Koschany [38]. Intermediate water removal in F1 reduces the presences of by-products. The reactors are simulated in Aspen Plus® as 'RPlug' with co-current thermal fluid and a specific heat transfer of 2,000 W $m^{-2}K^{-1}$. The inlet temperature is set to 250 °C and the flow of the thermal fluid is adjusted to reach a reactor outlet temperature of 283 °C. The thermal fluid is water at 280 °C and a pressure of 70 bar boiling in the shell side of the reactor. The vapor fraction of the water changes from 0 to 100 %. The reactors are simulated with tube diameter of 0.02 m. The first two reactors (R1 and R2) have a length of 5 m, reactor R3 has 3 m length. The number of tubes is adjusted to reach about equilibrium concentration at the outlet of each reactor. The catalyst bed voidage is set to 0.4 and a particle density is 336 kg m^{-3} with catalyst diameter of 0.003 m and the shape factor of 1.

For HSNG-mixtures at HSNG-10 and above, a H_2-bypass is added. Its flow is adjusted to reach the targeted concentrations presented in Table 1. Additional water removal at the end of the process is added. It is assumed in this publication, that the off-heat can be sold for district heating, thus is generating a revenue.

The chosen GHSV-values are attached in the SI in Table S9. In Tables S20 - S23, the temperatures and concentrations of the process streams are attached.

2.7. Technical key performance indicators

Technical key performance indicators, eq. (13) – (17), are used, as presented in Rahmat et al. [20].

$$\eta_{PtF} = \frac{\sum \dot{m}_{Synfuel} \bullet LHV_{Synfuel}}{\sum P_{el}} \tag{13}$$

The power-to fuel efficiency, η_{PtF}, includes the electrical energy flowing into the system, P_{el}, and the product flow $\dot{m}_{Synfuel}$, and the lower heating value of the product, $LHV_{Synfuel}$. Excluding the electrolyzer, the hydrogen to fuel efficiency, η_{HtF}, divides the energetic product output by the mass flow of hydrogen $\dot{m}$ and its lower heating value, LHV_{H_2} eq. (14).

$$\eta_{HtF} = \frac{\sum \dot{m}_{Synfuel} \bullet LHV_{Synfuel}}{\dot{m}_{H_2} \bullet LHV_{H_2}} \tag{14}$$

For further analysis, the exergetic efficiencies are calculated eq. (15) to (17).

$$\varepsilon_{PtF} = \frac{\dot{E}_{Synfuel}}{\sum \dot{E}_{F,i}} = \frac{\dot{E}_{Synfuel}}{\dot{E}_{Net,Electricity} + \dot{E}_{Net,\ Heat}} \tag{15}$$

In the power-to-fuel exergetic efficiency (ε_{PtF}) the amount of exergy in the synfuel $\dot{E}_{Synfuel}$ is compared to the input exergies. Here, $\dot{E}_{Net,Electricity}$, is the net exergy flow into the system minus generated electricity and $\dot{E}_{Net,Heat}$, the net heat flow into the system including the CO_2 extraction. The power-to-X (ε_{PtX}) exergetic efficiency, eq. (16), further considers that some of the wasted-exergy can be used ether as heat, $\dot{E}_{Heat,prod}$ or in by-products, $\sum \dot{E}_{By-product}$.

$$\varepsilon_{PtX} = \frac{\sum \dot{E}_{P,i}}{\sum \dot{E}_{F,i}} = \frac{\dot{E}_{Synfuel} + \dot{E}_{Heat,\ prod} + \sum \dot{E}_{By-product}}{\dot{E}_{Net,\ Electricity} + \dot{E}_{Net,\ Heat}} \tag{16}$$

Analogue to the η_{HtF} efficiency, the process-to-x ($\varepsilon_{Process-to-X}$) exergetic efficiency can be calculated, eq. (17), excluding the production of hydrogen and the purification of CO_2 and instead using the exergetic inflows of hydrogen $\dot{E}_{H_2}$ and carbon-dioxide, $\dot{E}_{CO_2}$. Furthermore, the electricity needed for the synthesis process, $\dot{E}_{Electricity,Plant}$, and generated electricity, $\dot{E}_{Electricity,generated}$ are considered.

$$\varepsilon_{Process-to-X} = \frac{\sum \dot{E}_{Process,\ Prod.,i}}{\sum \dot{E}_{Process,\ Fuel,\ i}} = \frac{\dot{E}_{Synfuel} + \dot{E}_{Heat,\ prod}}{\dot{E}_{H_2} + \dot{E}_{CO_2} + \dot{E}_{Electricity,\ Plant} - \dot{E}_{Electricity,\ generated}} \tag{17}$$

2.8. Economic assessment

Based on the methodology of Peters et al. [46] and adaptions of Albrecht et al. [47] and Maier et al. [48], a standard framework of assumptions for the economic analysis of PtX processes for German production was published by Heimann et al. [14] and is utilized in this paper. Assumed temperatures and pressures of the environment, H_2, CO_2 and water are attached in the SI in Table S7.

Labor costs were calculated using rules of thumb for labor hours estimation [46]; assuming large equipment, highly automated and estimating the number of production steps. Economic surcharge factors are listed in the SI in Tables S10-S11, raw materials and utilities are listed in Tables S12 and S13 and the calculated labor hours listed in Table S14.

2.8.1. Net production costs

An adapted cost calculation methodology based on works of Peters et al. [46] with adaptions by Albrecht et al. [47] is used. Methodology, assumptions and cost factors are described more detailed in Heimann et al. [14]. Net production costs (NPC) are calculated according to eq.

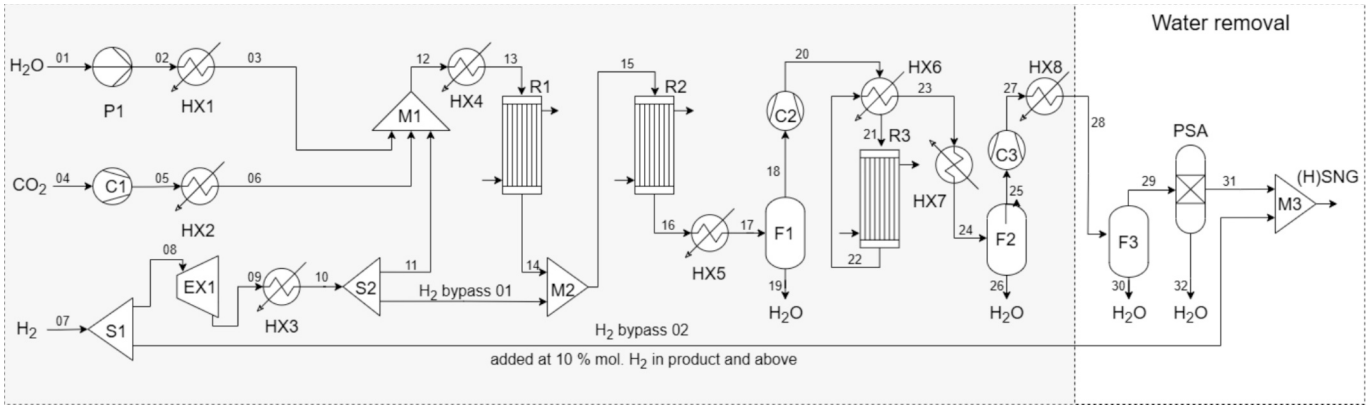

Fig. 2. Flow diagram of the isothermal methanation process for SNG and HSNG.

(18).

$$NPC\left[\frac{€}{MWh_{LHV}}\right]=\frac{ACC+\sum OPEX_{dir}+\sum OPEX_{ind}+t_{labor}\bullet c_{labor}}{\dot{m}_{synfuel}\bullet LHV_{synfuel}} \quad (18)$$

The operational expenditures (OPEX) consist of direct and indirect OPEX as in eq. (18). Direct OPEX are calculated using the energy costs and costs of raw materials as presented in Table 2 and in the SI for auxiliary materials in Table S12 and S13. The indirect OPEX are calculated with the help of surcharge factors as in Peters et al. [46]. Annual capital costs (ACC) are calculated as in eq. (19).

$$ACC=FCI\bullet\left(\frac{IR\bullet(1+IR)^{y}}{(1+IR)^{y}-1}+\frac{IR\bullet y}{(y-1)}\right) \quad (19)$$

Fixed capital investment (FCI) can be calculated using eq. (20).

$$FCI=\sum EC_i\bullet\left(1+\sum_{j=1}^{10}F_{eco,ij}\right)\left(1+\sum_{j=11}^{12}F_{eco,ij}\right) \quad (20)$$

The interest rate (IR) of 5 % and the plant operating time (y) of 20 years are assumed as in [14,20]. For equipment cost (EC_i), see eq. (21)

$$EC_i=f_i\left(S_{i,1},\cdots,S_{i,k}\right)\bullet\left(\frac{CEPCI}{CEPCI_{ref\ (i)}}\right)\bullet F_{material,i}\bullet F_{pressure,i}\text{for}\,i,k\in\mathbb{N} \quad (21)$$

The Chemical Engineering Plant Cost Index (CEPCI) [49] is used to account for inflation. Material and pressure factors $F_{material,i}$, $F_{pressure,i}$ are included depending on the equipment cost function. EC for standard equipment, e.g., flash drums, pumps, turbines, compressors, heat-exchangers and blowers are estimated based on [46]. The cost for the steam generator was taken from Hannula [50]. The steam cycle was adopted from Hamelinck et al. [51] and the adiabatic fixed bed reactor and multi-tubular bed reactors from Woods [52]. Materials are selected by temperature as in [14], see Table S15. Heat exchanger sizes and sources for cost functions are listed in the SI in Tables S24-S31. The adiabatic plug-flow reactor for TREMP is calculated according to [52] and made from nickel-alloy. Separators (flash) are calculated according to Peters et al. [46] using stainless steel. The isothermal plug flow-reactors R1, R2 are calculated using Woods [52] with steel 1.4401, the isothermal R3 is calculated using [46] and the same material. Total capital investment (TCI) is calculated using eq. (22) and a working capital of 15 % [47].

$$TCI=\frac{FCI}{1-workingcapital} \quad (22)$$

3. Result and discussion

In the next chapters, the technical and economic analysis results are presented.

3.1. Technical results

Fig. 3 shows the power-to-fuel-efficiencies at various H_2 concentrations for both process configurations and the HSNG-cases.

Under the given assumptions, η_{PtF} is about 57 % for the SNG of TREMP and about 45 % for the isothermal process. This small difference is due to the generated electricity in TREMP which reduced the overall amount of needed electrical power. Increasing the amount of hydrogen in the synfuels, reduces the chemical conversion losses. For HSNG-30, the efficiency is 83 % for TREMP and 56 % for the isothermal process. There seems to be a linear dependency on of η_{PtF} to the H_2 content of the final product which can be explained by the reduction of synthesis losses. The efficiency η_{H_2tF} for SNG is identical for both processes at about 83 % for the SNG case which is the value of the theoretical efficiency and about 85 % at HSNG-30. This is due to the comparison of only chemical energy flows with no purges and identical target purities. A list of all KPI is attached in Table S32 of the SI.

3.1.1. Exergy analysis

An overview over the exergy-streams of the SNG production is given in the Sankey diagrams with input exergy flows set to 100 %, Fig. 4.

For TREMP the recycled electricity generated by the steam cycle is included in the 100 % Input exergy. Therefore, the primary electrical energy demand is lower. The highest share of exergy destruction is caused by the electrolysis. Here about 30 % of its exergy input is destroyed. The CO_2 capture process is substantially less efficient, with an exergy destruction of 69 % of its input. However, the exergy input for both methanation processes is composed of about 98 % exergy from hydrogen and 2 % exergy from carbon dioxide, making the electricity requirements of the synthesis processes negligible. In the synthesis about 5 % of exergy is destructed or lost for TREMP and 7 % in the isothermal process.

Within the synthesis processes, only a small portion of the primary exergy is lost as can be seen in the $\varepsilon_{Process-to-X}$ exergetic efficiency. It is in the range of 93 % (SNG) to 94 % (HSNG-30) for TREMP and of 89 % (SNG) to 90 % (HSNG-30) for the isothermal process. For the whole process including the electrolyzer and CO_2-extraction, the ε_{PtF} is about 57 % for TREMP and 55 % for the isothermal process, respectively, for SNG. For HSNG-30 it reaches up to almost 58 % for TREMP and 56 % for the isothermal process. This exergetic efficiency gives an insight into the

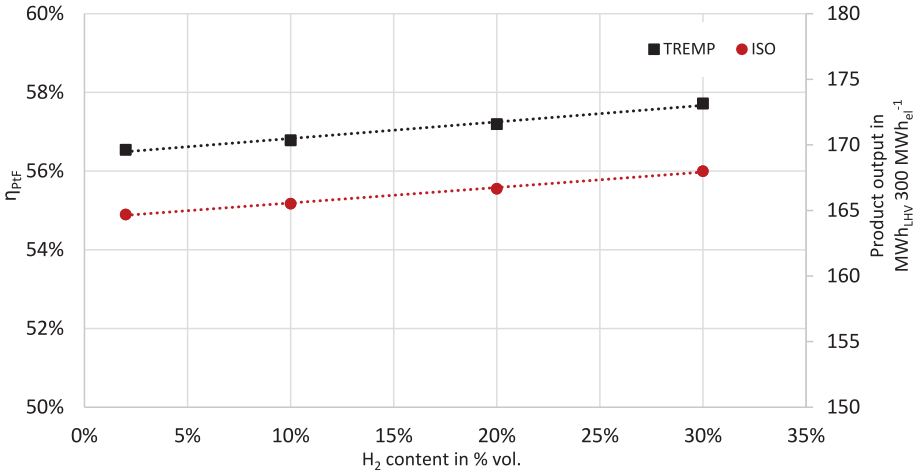

Fig. 3. Power-to-fuel-efficiency at different H_2-concentrations for TREMP and isothermal process. Linear interpolation added.

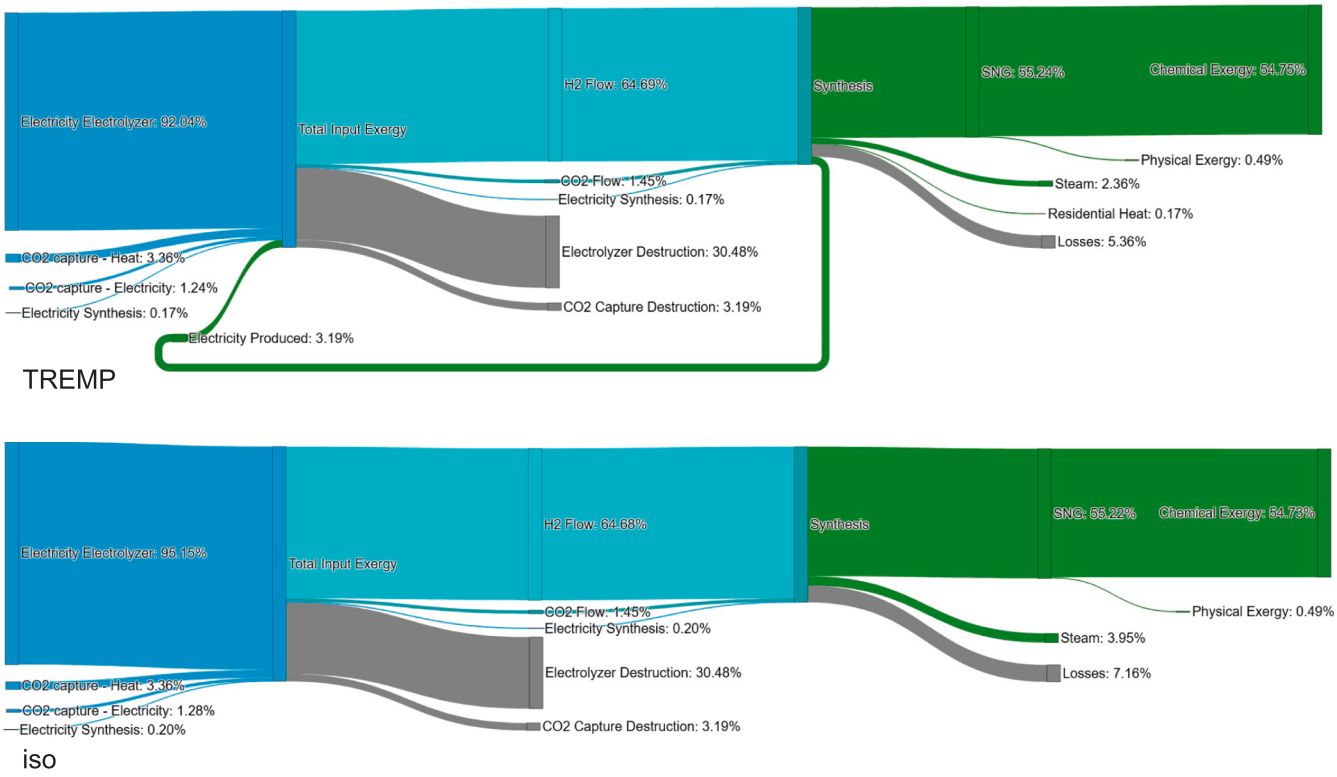

Fig. 4. Sankey diagram of exergy flows for SNG.

primary exergy which can be used in the product. If waste-heat can be sold, the exergetic efficiency, ε_{PtX}, increases up to about 60 % for TREMP and the isothermal process with only slight changes for different H_2 concentration. The process performance can be assessed by $\varepsilon_{Process-to-X}$, which is about 91 % (SNG) to 92 % (HSNG-30) for TREMP and 90 % for the isothermal processes. In all efficiencies, a linear dependency on the products hydrogen content could be observed. A list of all KPI is attached in Table S18 the SI.

3.2. Economic analysis

The production of SNG or HSNG-blends can only be competitive on the market, the production costs are close to market prices or if other benefits are corelated with the product. In the next chapters, the costs are analyzed.

3.2.1. Fixed capital investment

The FCI for each product concentration is divided by the energy flow of the product, based on its lower heating value. This allows for an energy-based comparison. In Fig. 5 the specific FCI for both production processes at different hydrogen concentrations is displayed.

Both processes are close together, so that the specific FCIs are within each other's the error margin. Nevertheless, there seems to be the trend of a specific cost reduction at higher hydrogen concentrations for TREMP whereas the specific FCI of the isothermal process change hardly.

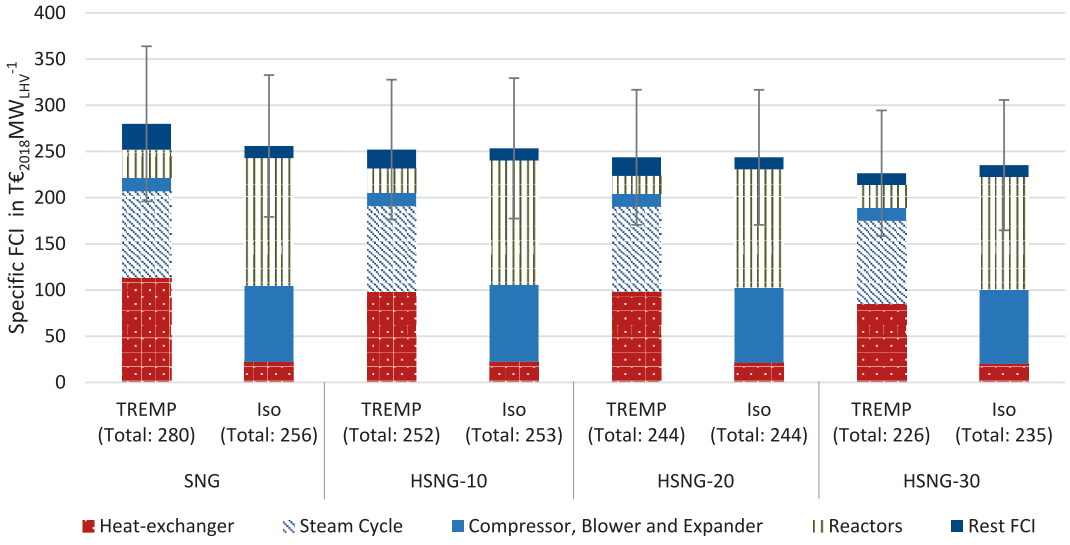

Fig. 5. Composition of the product specific FCI for 5 $t_{H2}h^{-1}$.

In TREMP, the heat integration contributes to about 41 % to the specific FCI for the SNG-case and the steam cycle to about a third of the specific FCI. This is due to the high temperatures at which the heat is being transferred. For HSNG-30 the specific FCI is reductions by about 19 % compared to SNG. This is due to the reduction of the number of reactors and smaller heat-exchangers. Specific FCIs of the steam cycles change hardly with higher hydrogen concentrations in the final product since the amount of heat which can be utilized rom HX3 is almost the same in all processes. This is due to the fact, that the first reactor always reaches the equilibrium at 700 °C. The specific FCI for the reactors reduces from SNG to HSNG-20 by about 37 %. For HSNG-30 the specific reactor costs increase compared to HSNG-20 since reactor 3 (R3) has to run at higher temperatures for the desired product specification. Nevertheless, for HSNG-30 two heat exchangers and a flash separator could be saved and the reactor is overcompensated. All changes are within the error margin of the cost calculation methodology.

In the isothermal process, the highest share of specific FCI lays within the tube bundle reactors which also function as heat exchangers. They account for about 54 % as seen in Fig. 5.

In the isothermal process the specific investment for the compressors, blower and expander are more than five times the value in comparison to TREMP. This is due to the higher number of compressors in the isothermal process. Due to the volume reduction within the methane production, the reactor sizes reduce only about 7 % in between SNG and HSNG-30. This results in specific FCI of the reactors being about 12 % lower at HSNG-30 in comparison to SNG production. Compressor-, blower- and expander-FCIs are about 2 % lower and the remaining heat exchangers at −9 %. Savings are within the margin of error of the methodology.

3.2.2. *Net production costs*

The NPC of TREMP and isothermal process are depicted in Fig. 6. There seems to be a linear dependency of the NPC on the hydrogen concentration of the product corresponding to η_{PtF}. The difference between TREMP and isothermal is at a magnitude of around 2.5 % in favor of TREMP.

Nevertheless, the chosen process has less influence on the NPC than the charges an levies on the energy which are the difference between the higher and lower electricity costs.

The main contributor to the production costs are hydrogen followed by carbon dioxide. Costs of H_2 and CO_2 are about 100 % of the NPC of TREMP. The other costs and revenues even each other out under the analyzed conditions. This means, that for this process under the given conditions, only energy costs define the overall NPC. In the isothermal process the costs of H_2 and CO_2 account for about 98 % of the total NPC. Here, the CAPEX has some influence on the products cost, since the process is not as efficient. The minor role of the CAPEX underlines the importance of optimized usage of excess heat. The presented results are for the case of demand for heat in close proximity. An ideal solution for each location has to be found individually. Fig. 7 indicates the NPC for the analyzed cases in comparison with an e-methanol production [20] and fossil counterparts (see also Table S33 of the SI).

For 2018 the NPC of SNG this is about 6 % to 11 % lower than in the synthetic methanol production, presented by Rahmat et al. [20] and close to Gorre et al. [15] for their calculation for 2017. Nevertheless, Gorre et al. [15] did not specify the product quality.

The NPC for TREMP and the isothermal process are close, with slightly higher NPC for the isothermal process. For *Case 1*, the net production cost decrease for future years due to the assumed lower electricity prices, rising electrolyzer efficiencies and thus, lower H_2-costs. The effect of the assumed rising CO_2-cost, is neglectable, since it has a low share of the overall costs. In *Case 2* with purchase agreements, the NPC are less than half of the NPC for *Case 3* locations without grid connections. Here, effects of low electricity demand during the Covid19 pandemic in 2020 with exceptionally low electricity costs can be seen. Nevertheless, the NPC are still about seven times more expensive than market prices of fossil counterparts. On the contrary, in isolated locations, the effect of the additional costs for energy-storage, curtailment and over-dimensioning of the electrolyzer can be seen with NPC about three times higher than a production with assumed purchase agreements. For comparison, the NPC for an e-methanol production under the same conditions is between 3 % and 18 % higher than the NPC of

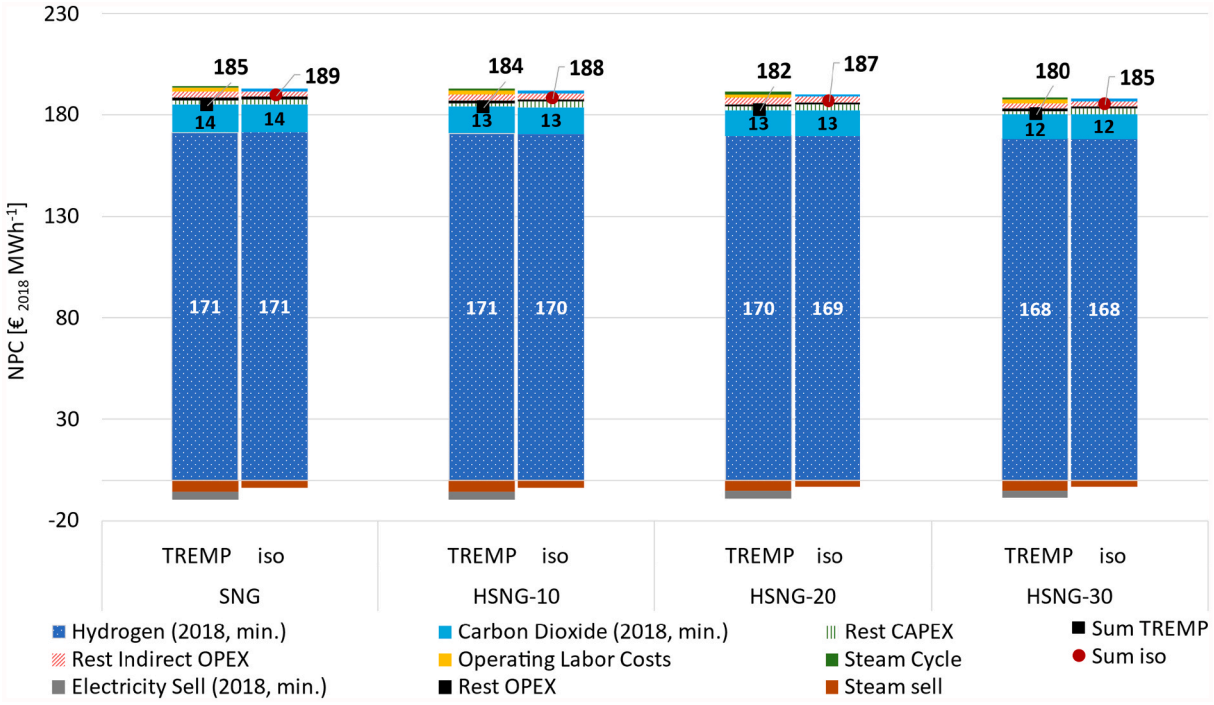

Fig. 6. NPC_{TREMP}, NPC_{ISO} of SNG and HCNG mixtures, 2018. (4.74 €$_{2018}$ kg$^{-1}_{H2}$, 68.95 €$_{2018}$ t$^{-1}_{CO2}$).

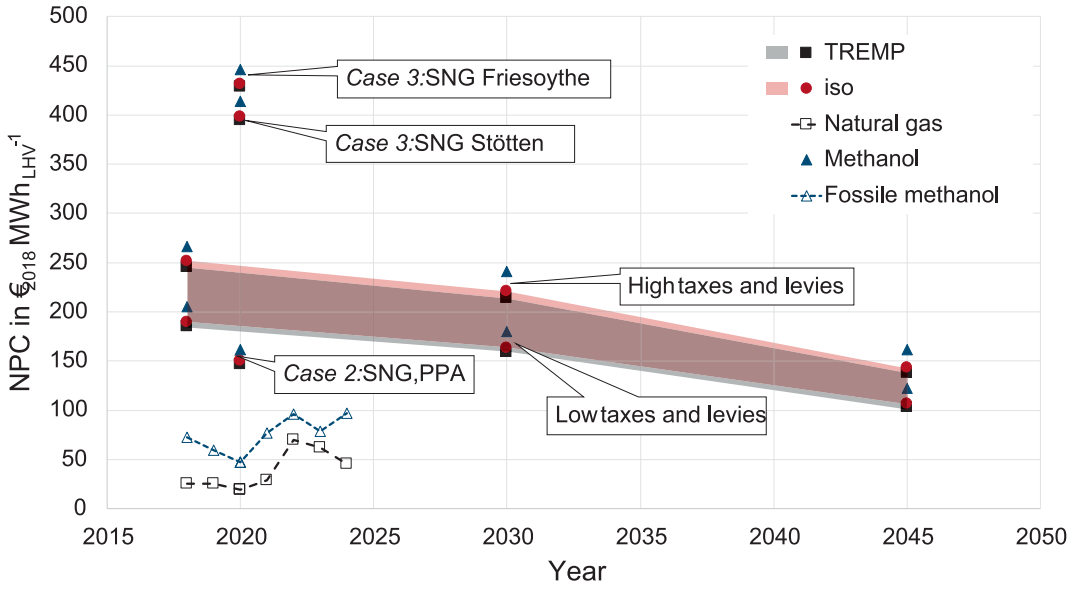

Fig. 7. NPC of SNG for analyzed years with upper and lower costs. Comparison with market prices of natural gas[a)] [53] and fossil methanol[b)] [54]. a) Consumption from 100 000 GJ to 999 999 GJ - band I4 [53]. b) Methanex European Posted Contract Price [54].

TREMP. In the methanol process, a purge is required to reduce the build-up of inert gasses. The losses of H_2 and CO_2 contribute to the extra costs. The easier separation of the gas SNG from its by-products in comparison to methanol which needs to be separated in a multi-column rectification might be an additional explanation. In Fig. 8 the NPC for a production in 2020 at different German locations is compared.

3.2.3. *Sensitivity analysis*

For better insight into these results, a sensitivity analysis is performed considering the influence of hydrogen and carbon dioxide cost. Fig. 9 and Fig. 10 show the sensitivity results for TREMP and the isothermal process, respectively. For a comparison: the price of industrial natural gas in Europe was 25.6 $€_{2018}$ MWh_{LHV}^{-1} in 2018 [55]. Using a similar heuristic approach as Rahmat et al. [20] the results are compared to the natural gas price and categorized in three groups: Competitive (below 150 % of the market price of the year 2018, i.e., 38.4 $€_{2018}$ MWh_{LHV}^{-1}, marked in green), presumably competitive (below 250 % of the market price, i.e., 96 $€_{2018}$ MWh_{LHV}^{-1}, marked in yellow) and not competitive (above 250 % of the market price, marked in red). These limits have been set arbitrarily. The equivalent cost for the threshold of 38.4 $€_{2018}$ MWh_{LHV}^{-1} with hydrogen price of 1.35 $€_{2018}$ kg^{-1} seems to not be realistic yet.

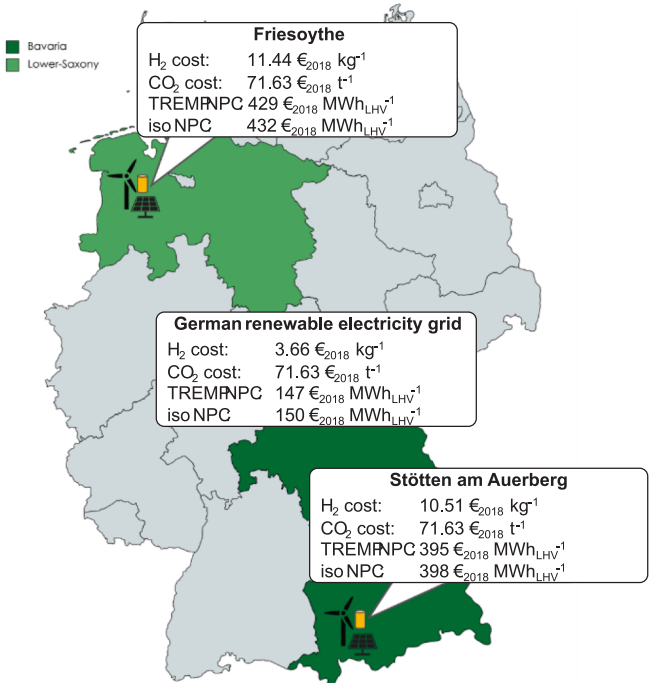

Fig. 8. Map: Case study of SNG production in Germany 2020.

Under the given circumstances and the relative production of electricity and energy for district heating, the NPC of the sensitivity study for TREMP of the reported size can be approximated with the following empirical equation (23).

$$NPC_{TREMP}\left[\frac{€_{2018}}{MWh_{LHV}}\right] = 0.197 \cdot CO_{2\,Cost}\left[\frac{€_{2018}}{t}\right] + 36.141 \cdot H_{2\,Cost}\left[\frac{€_{2018}}{kg}\right] + 0.939 \quad (23)$$

Under the given circumstances and the relative production of sellable steam, the NPC for the isothermal-process of the reported size can be approximated with the empirical equation (24).

$$NPC_{ISO}\left[\frac{€_{2018}}{MWh_{LHV}}\right] = 0.196 \cdot CO_{2\,Cost}\left[\frac{€_{2018}}{t}\right] + 36.131 \cdot H_{2\,Cost}\left[\frac{€_{2018}}{kg}\right] + 4.262 \quad (24)$$

In comparison to the methanol production, as presented in Rahmat et al. [20], a sensitivity for the CO_2 costs at a constant hydrogen cost is presented in Fig. 11 since there seems no difference in the sensitivity towards the hydrogen cost between methanol and SNG production.

As indicated, the NPC of methanol is higher than those of the methane processes for all hydrogen costs. The relatively high sensitivity towards the CO_2 costs originates in the purge in the methanol process and with that a slightly higher CO_2 demand per unit of energy. There is no purge in the analyzed SNG processes.

4. Energy decarbonization scenarios using SNG and HSNG

Despite the high cost of SNG or HSNG compared to fossil natural gas or imported LNG, a market introduction might be worth to consider as an option for increased energy security, independence and sustainability while widely using existing infrastructure. SNG and HSNG can be

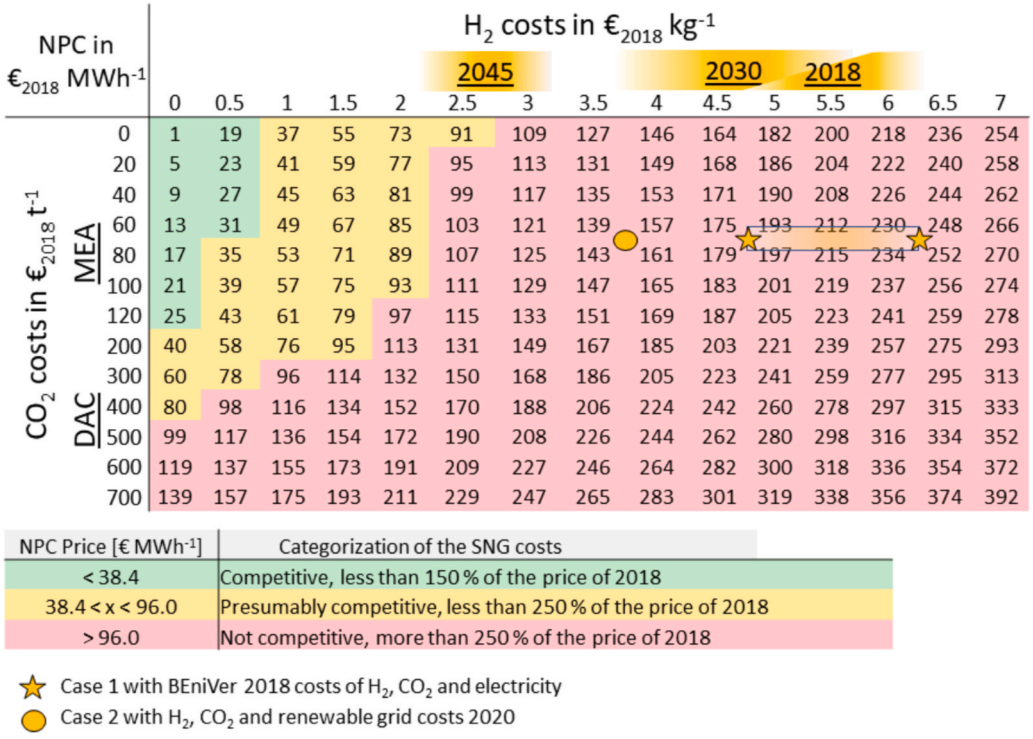

Fig. 9. Sensitivity of $NPC_{SNG\text{-}TREMP}$. (Assumed process electricity cost 42 $€_{2018}$ MWh_{LHV}^{-1}).

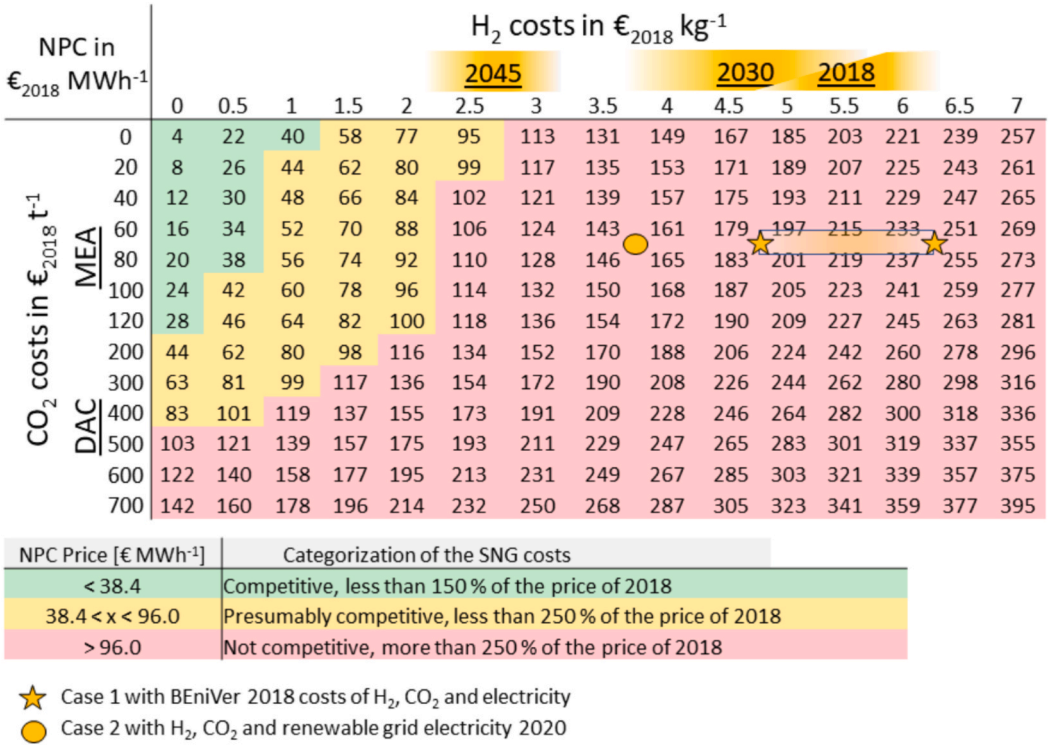

Fig. 10. Sensitivity of $NPC_{SNG\text{-}iso}$. (Assumed process electricity cost 42 $€_{2018}$ MWh_{LHV}^{-1}).

produced with low climate impacts compared to the fossil counterparts and could be introduced in an existing gas grid capable of transporting and storing huge amounts of energy. The resilience of the highly interconnected natural gas grid could be used making the energy supply more secure. Since transporting energy through the gas grid is about one tenth of the cost of electricity transport [56], huge investment would be needed for direct electrification. Therefore, chemical energy carriers will probably still play a role in future. Current EU strategy to focus solely on hydrogen bears the risk of parallel structures of natural gas and hydrogen or of insufficient supply to customers as projection suggest. In German for instance, more than 160 TWh of industrial thermal energy demand is further than 1 km away from the planned German H_2-core-

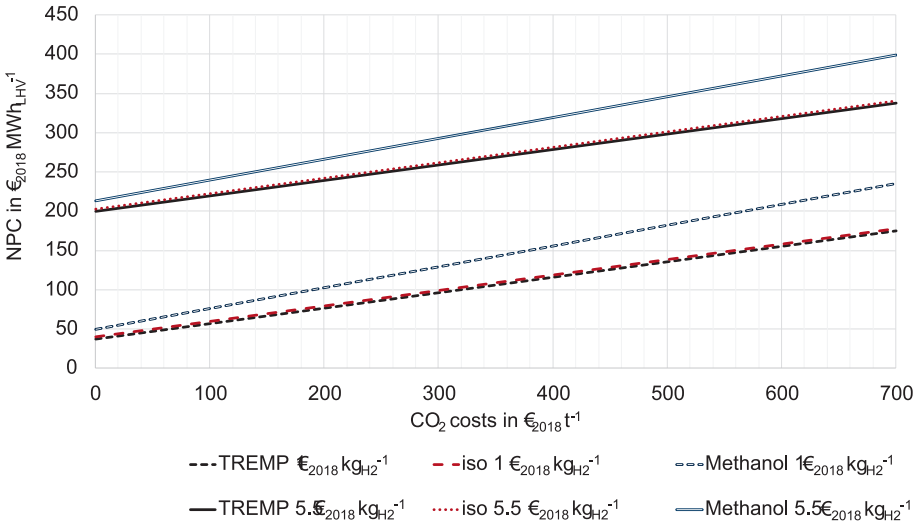

Fig. 11. Sensitivity study of NPC for SNG and methanol [20] at 1 and 5.5 $€_{2018}$ kg_{H2}^{-1}.

network, [57]. Furthermore, a large share of private customers rely on natural gas for their heating. All of these customers have to be connected to a new hydrogen grid or use other means of heating. Furthermore, it is doubted by the European court of auditors, that proposed EU hydrogen supply goal for 2030 could be reached [58]. In order not to wait until there is enough H_2 available and all the infrastructure is changed completely, there might be a path where CO_2-emmision-savings can be implemented fast and a change to 100 % renewables is possible. Utilizing several energy sources and, probably, hydrogen-methane-blends could foster a robust transition which is less susceptible to global crisis. Using SNG and HSNG for industry, households and transport applications allows for synergies, especially in the use of infrastructure and usage of waste-heat. Adapting the gas grid and energy sources in realistically planned single steps has a higher likelihood of success than a complete switch in a short period of time. In the next section technical feasibilities for methane-hydrogen blends and 100 % hydrogen are presented.

4.1. Gas grid

While both the European and the German strategy for decarbonization only considers electrification and hydrogen, it's implementation will cause the waste of enormous legacy infrastructure of 2 Mkm natural gas distribution network in Europe which has an approximated investment of about 5 BN€ [59] and a storage capacity of about 1,700 TWh [60]. Despite current discussion of the use of hydrogen, methane is still advantageous for the transport and use in the industry.

4.1.1. Technical feasibility of the usage of HSNG in the gas grid

There already have been discussions on using the existing grid for natural gas-hydrogen-blend [11]. In the SI in Table S34 key findings of several publications considering the influence of hydrogen admixtures on the gas grid and on customers is summarized.

As prove of concept of hydrogen-natural-gas-blends in the gas grid, Netze BW, a German gas distribution system operator, tested the feed-in of up to 30 % vol. H_2 in the "Hydrogen Island Oehringen" project, from 2021 to the end of 2023 in Baden-Württemberg. Initially, the company's own operations center was supplied with 10 to 30 % hydrogen, which was then fed into the grid to the end user. The appliance test showed that all indoor appliances were suitable for mixed gas operation with up to 30 % H_2 by volume. All gas appliances were suitable for up to 15 % vol. H_2, some of which were classified capable up to 30 % vol. H_2. During the project, 6 of 30 appliances, 20 %, were replaced for reasons of safety and security which is significantly less than the replacement considering direct electrification. No failures due to H_2 admixture occurred during the feed-in phase which seems to prove the robustness of the gas grid and its components [11]. For more information on specific components see also DVGW e.V. [61].

4.1.2. Costs for the transformation of the gas infrastructure

The investment and changeover planning represents an important step towards concretizing the transformation plans. Technical concepts and resulting costs were examined in the DVGW project "Roadmap Gas 2050″ [61], with a focus on the comparison of different variants for Germany-wide transformation paths with different target values and implementation speeds, as well as various subsequent projects both in the field of research and in the context of services for network operators.

The costs for the transformation of the German gas grid are approximately 9 % higher than those required for regular renewal due to age and wear, considering a reduction in household gas connections to 67 % and network length to approximately 80 % by 2045. The greatest need for adaptation is in the area of measurement technology and gas pressure control [61]. Similar orders of magnitude are the result of network operator-specific considerations. In general, most of the costs are incurred for replacing the gas applications. For a blending scenario of 20 % vol. H_2 by 2035, the additional costs are about 31 billion €. For a blending of 30 % vol. H_2 by 2035, the additional costs are around 48 billion € which is close to the 56 billion € for a 100 % hydrogen grid [61]. Adapting the gas grid with various blending options on the way to conversion, tend to lead to slightly higher costs, as some components such as meters or gas applications may have to be replaced several times. A transition to 20 % vol. H_2 in the gas grid or directly 100 % H_2 seem to be the most economic solutions.

4.1.3. Regulatory framework

Converting gas networks is a complex process, especially in the lower network levels, where the degree of meshing is higher and many customers are connected. Lower hydrogen concentrations, especially $\leq$ 20 % vol., tend to have less hurdles. All of the necessary steps are known and are subject of current research as highlighted in the previous chapters. Further analysis needs to be carried out. In each step, an authorized expert must be involved in the assessment of the network [62]. It is then necessary to define specific sub-networks for the changeover, including the sequence and determination of the measures required for this, including planning the adjustments to the network to establish H_2 readiness. The conversion requires a temporal disconnection of the network components and a definition of the conversion areas depending on the available personnel in order to limit the supply

disruption for customers.

The limits of the admixture of hydrogen to methane are defined by the DVGW regulations, in particular G260 (gas quality) [22] and G 685 (gas billing) [63]. Blending within this limits does not require notification or approval. Below 20 % vol. H_2 admixture needs no permission if the infrastructure is capable of handling the concentration. The capabilities of the infrastructure has to be enquired about with the network operators concerned if there is a request to feed in hydrogen.

A conversion to hydrogen must be notified to the relevant authorities (113c EnWG [64]) and approval may also be required if significant changes to the pipeline or grid take place. An admixture that exceeds the limits of the currently valid DVGW regulations needs a framework to be created.

4.1.4. Proposing a smooth transition from a natural gas supply towards gradual H_2 and SNG inclusion

Given the limited hydrogen supply, technical economical and regulatory frameworks, a transition of the gas grid in two mayor steps might be a good pathway for a de-fossilization of the gas grid. In Fig. 12 an idea for a stepwise adaption of the gas grid is proposed.

By a mandatory admixture of 20 % vol. H_2 to the gas grid by, for instance, **2030**, the CO_2 emissions could immediately be reduced by about 7 %. For Germany this required up to 314 TWh a^{-1} H_2 if no biogas and SNG/HSNG where available and with a gas usage of 844 TWh as in 2024 [65]. Still, this exceeds the assumed German H_2 demand by 2030 of about 130 TWh a^{-1} [66]. This highlights once more the huge transition which has to take place. Going for 100 % hydrogen would require significantly higher hydrogen supply. The step of admixing up to 20 % vol. H_2 to the gas grid could take place if the hydrogen supply is secured which means about 100 GW electrolyzer capacity for Germany alone. Further energy sources could be tapped by an increased use of upgraded biogas to the limits which are sustainable. These could reach up to 116 TWH today and 113 TWh [67] by 2045 which is about 13 % of the current German natural gas usage. Excess CO_2 could be utilized by the production HSNG-20 to further reduce the need of natural gas. By **2032**, when the German H_2 backbone is planned on being finished, local gas grids can be converted to 100 % H_2 if sufficient hydrogen is available. Further reduction could be achieved by increasing efficiencies, direct electrification and local heat networks. By **2045** this process of converting local gas grids is finished. Probably there might be local use of biogas remaining or of HSNG or SNG for specialized applications. Using this path, there is still the possibility for adaptions on the path to a 100 % renewable gas grid and the network might have a higher resilience.

4.2. Application of synthetic natural gas and hydrogen-synthetic natural gas in the transport sector

Changing the transport sector to renewables requires to increase the use of electrified transport as it is the method with the highest efficiency. This comes with a need of heavy investment in renewable power production and charging infrastructure. Nevertheless, non-electric mobility will sustain for many years and requires an additional decarbonization strategy. Within the project MethQuest, a German methane demand of 100–140 TWh was predicted in different scenarios, mainly for trucks and passenger cars, less for marine applications [13]. Taken the production cost for data of Fig. 7 that would cause about 10.3 – 19.3 Bn. € for SNG and 9.9 – 18.8 Bn. € for HSNG-30 in 2045, compared with approximately 10.9 Bn. € for gasoline and 19.6 Bn. € for diesel in 2023 [68,69]. With 780 tank stations in Germany in 2023 and operation for over 20 years, there is enough experience about the logistics and applicability of CNG in transport [70]. However, despite the ecological advantage of CNG compared to gasoline/diesel, even larger ecological advantage for biomethane and the potential production of SNG with renewables, the relevance of CNG in Germany was always negligible and is further fading away. It is possible to retrofit gasoline cars to run on SNG or HSNG-blends but only tax stimulation can force the limitation of fossil gasoline and diesel consumption. The most energy-efficient and therefore most affordable synfuel would be HCNG-30 in any calculation. It could be applied in shipping and long-distance freight sector, for ambulances and fire engines, construction vehicles and excavators. If future fuels are made mainly from renewable electricity, HCNG-30 could be the fuel of choice for all non-electric transport except current aviation.

Within the project CombiFuel [71] an alternative HSNG production method was proven. An application of plasma to reduce the carbon- and nitrogen load of sewage, simultaneously producing methane and hydrogen has been shown. After separating these gases from N_2 and CO_2, the produced HSNG can be directly used as a renewable fuel. Currently, there is a plant running and fueling the fleet of Graforce GmbH [72]. That shows, with sufficient political support and incentives, HCNG-30

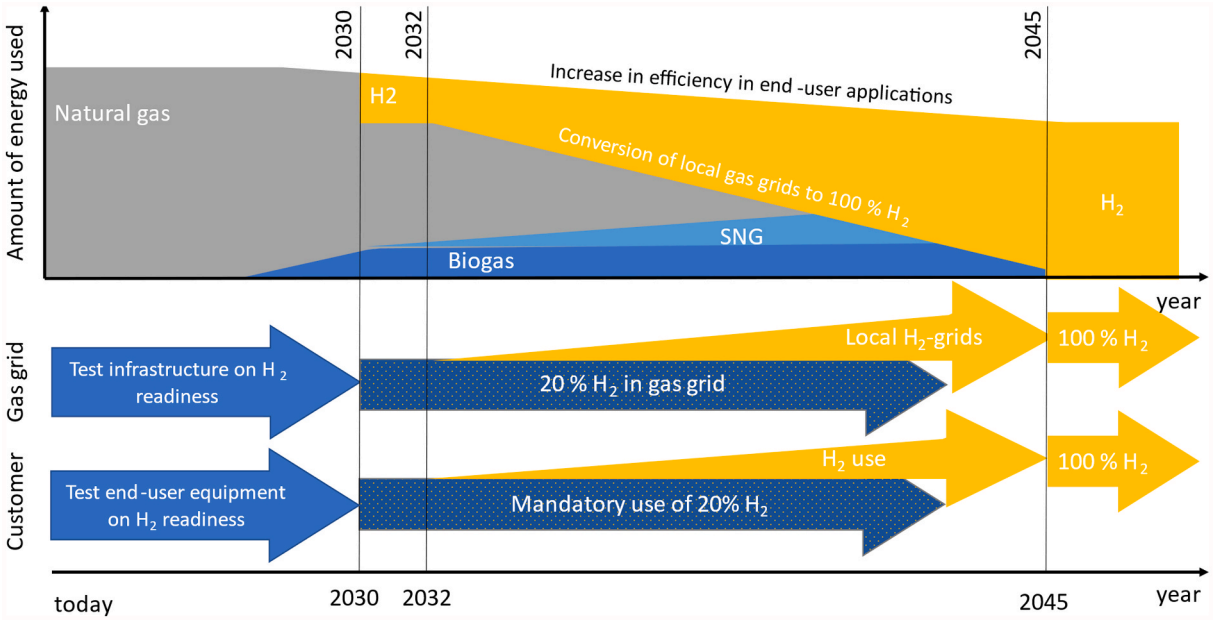

Fig. 12. Possible adaption scenario for the gas grid. (Not to scale.)

usage in transport might be developed using diverse feedstock sources, as even biomethane could be mixed with hydrogen from renewable electricity.

A detailed cost and benefit assessment require a detailed life cycle analysis, of production, logistic and usage, the cleaner burning characteristic in internal combustion engines as well as potential methane slip on the entire supply chain and the usage. This exceeds the scope of this article and could be the topic of a subsequent one later.

5. Summary and conclusions

SNG is the carbon-based PtX with the highest synthesis efficiency of about 83 % (η_{H_2tF}). It has good storability, can be utilized in existing infrastructure and is applicable for both the energy- and the transport sector. Domestic production of SNG could support climate neutrality and increase energy security and independence. The SNG product specification of this publication could be used as well in the gas grid as in the transport sector.

The comparison of a high- and a low temperature production process shows a slightly higher η_{PtF} (+1.6 %) for TREMP. In the base-year 2018, the NPC for SNG is about 185 to 245 $€_{2018}$ MWh^{-1}_{LHV} (TREMP) and almost the same for the isothermal process at about 189 to 251 $€_{2018}$ MWh^{-1}_{LHV}. The higher exergetic efficiency in TREMP improves the usage of the costly hydrogen, however slightly higher CAPEX and higher workforce almost level this advantage out.

A case-studies using only locally sourced renewables with no grid connection including a hydrogen storage, curtailment, dimensioning of the electrolyzer, wind farm, photovoltaics, using the methodology of Raab et al. [27], show much higher NPC. The calculated NPC for 2020 range between 429 $€_{2018}$ MWh^{-1}_{LHV} (TREMP) and 432 $€_{2018}$ MWh^{-1}_{LHV} (iso) for Friesoythe and between 429 $€_{2018}$ MWh^{-1}_{LHV} (TREMP) and 398 $€_{2018}$ MWh^{-1}_{LHV} (iso) for Stötten. In comparison a possible German renewable electricity price with PPA at the exceptionally low day-ahead prices of 2020 has been calculated, resulting in NPC of 147 $€_{2018}$ MWh^{-1}_{LHV} (TREMP) and 150 $€_{2018}$ MWh^{-1}_{LHV} (iso), which is still about seven times the fossil natural gas price of that year. A sensitivity study suggested that with hydrogen costs less than 1.35 $€_{2018}$ kg^{-1}_{H2} the NPC of 150 % of the fossil natural gas might be reachable which seems not realistic today. The CO_2 costs have a minor effect on the NPC as they only account for about 8 % of the total NPC.

A NPC comparison of e-methanol production [20] suggests that synthetic methanol might be about 3 % to 18 % more expensive than SNG.

A further analysis for HSNG-blends up to 30 % H_2 vol. shows a simplified TREMP process with less reactors and a decrease of the specific FCI by 19 % for HSNG-30 compared to SNG. The specific FCI of the isothermal process could be reduced less than 0.5 % as a bypass-compressor has to be included. A 10 % vol. H_2 increase can result in about 0.4 % higher η_{PtF} for both processes and about an NPC reduction of about 1.7 $€_{2018}$ MWh^{-1}_{LHV} (TREMP) and 1.6 $€_{2018}$ MWh^{-1}_{LHV} (iso) for minimal taxes and levies.

Allowing higher hydrogen shares in the gas grid could not only simplify possible production processes but could also allow for stepwise integration of hydrogen production capacities in a nationwide gas grid. In the transport sector, HSNG could increase motor efficiency, improve exhaust qualities and lower CO_2 emissions. A sweet spot seems to be at 20 % vol. H_2 where technical and economical expense for the adaption of the gas grid and end-user appliances are comparably low.

6. Outlook

Of the synthetic carbon-based chemical energy carrier, methane and methanol should be preferred for hard-to-abate sectors. The low hydrogen concentration in current natural gas standards results in high effort in the process configuration driving up SNG production costs. Increasing the allowable hydrogen content in the gas grid and introducing HSNG into the transport sector in the near future could offer positive effects on the sustainability of energy supply by limiting the risks and costs while utilizing the existing infrastructure and user applications.

Locally available renewable CO_2 and local heat demand should be considered for possible SNG production sites. An assessment on load following capacity of TREMP and the isothermal process could be done to improve cost calculations for fluctuating renewable energies. The use of low-temperature heat of electrolyzers might be considered in future to lower NPC.

To introduce the technology at large scale, several 300 MW electrolyzers and synthesis plants would have to be built. Even though there is a ramp up of large electrolyzer production capacities as reported by the Hydrogen Council [73], the needed capacities seem currently hard to achieve in the short run. Furthermore, the additional demand of renewable energy, cables and electronics has to be met. Further analysis of aspects related to society and politics should be carried out as well.

CRediT authorship contribution statement

Nathanael Heimann: Writing – review & editing, Writing – original draft, Visualization, Methodology. **Francisco Moser:** Writing – original draft, Validation, Methodology. **Moritz Raab:** Software, Methodology. **Jens Hüttenrauch:** Writing – original draft, Validation. **Ralph-Uwe Dietrich:** Writing – review & editing, Supervision, Conceptualization.

Declaration of competing interest

The authors declare that they have no known competing financial interests or personal relationships that could have appeared to influence the work reported in this paper.

Appendix A. Supplementary data

Supplementary data to this article can be found online at https://doi.org/10.1016/j.enconman.2025.120973.

Data availability

Data will be made available on request.

References

[1] UNFCCC (2015): *The Paris Agreement* [accessed 04-19-2022]. Available at: https://unfccc.int/process-and-meetings/the-paris-agreement/the-paris-agreement.
[2] IEA (2025): Global Energy Review 2025. [accessed 08-29-2025]. Available at: https://www.iea.org/reports/global-energy-review-2025.
[3] European Commission J.R.C.C., M.; Guizzardi, D.; Pagani, F.; Banja, M.; Muntean, M.; Schaaf, E.; , Monforti-Ferrario F.B., W.E.; Quadrelli, R.; Risquez Martin, A.; Taghavi-Moharamli, P.; Köykkä, J.; Grassi, G.; Rossi, S.; Melo, J.; Oom, D.; , Branco A.S.-M., J.; Manca, G.; Pisoni, E.; Vignati, E.; Pekar, F (2024): *GHG emissions of all world countries*. Publications Office of the European Union L. [accessed: 07-13-2025] Available at: https://data.europa.eu/doi/10.2760/4002897.
[4] Dietrich R.-U., Adelung S., Habermeyer F., Heimann N., Maier S., Raab M., Rahmat Y. (2025): *Fuels – Introduction | Hydrogen Non-Conventional Storage Options*, in: Garche J., (Ed.): *Encyclopedia of Electrochemical Power Sources (Second Edition)*, Elsevier. Oxford: 199–231. ISBN 978-0-323-95822-6. doi: https://doi.org/10.1016/B978-0-323-96022-9.00183-3.
[5] Rönsch S, Schneider J, Matthischke S, Schlüter M, Götz M, Lefebvre J, et al. *Review on methanation – from fundamentals to current projects.* Fuel 2015;166:276–96. https://doi.org/10.1016/j.fuel.2015.10.111.
[6] Bundesnetzagentur (2024): *Hydrogen core network*. [accessed: 10-24-2024] Available at: https://www.bundesnetzagentur.de/EN/Areas/Energy/HydrogenCoreNetwork/start.html.
[7] CNG-Mobilität *Boom in Deutschland dank LKW*. sd. [accessed: 02-27-2025] Available at: https://www.cng-mobility.ch/beitrag/boom-in-deutschland-dank-lkw/.
[8] Luo S, Ma F, Mehra RK, Huang Z. *Deep insights of HCNG engine research in China.* Fuel 2020;263:116612.
[9] DBFZ Deutsches Biomasseforschungszentrum gemeinnützige GmbH (2021): *DBFZ Report Nr. 44 - Monitoring erneuerbarer Energien im Verkehr* (Ed. Jörg Schröder K.N.). DBFZ Deutsches Biomasseforschungszentrum gemeinnützige GmbH. doi: 10.48480/19nz-0322.

[10] American Bureau of Shipping (20222): *LNG AS MARINE FUEL*. SUSTAINABILITY WHITEPAPER.

[11] Netze BW GmbH (2024): *Wasserstoff-Insel Öhringen*. [accessed: 12-20-2024] Available at: https://www.netze-bw.de/unsernetz/netzinnovationen/wasserstoff-insel.

[12] Dimopoulos P, Rechsteiner C, Soltic P, Laemmle C, Boulouchos K. *Increase of passenger car engine efficiency with low engine-out emissions using hydrogen–natural gas mixtures: a thermodynamic analysis*. Int J Hydrogen Energy 2007;32(14): 3073–83. https://doi.org/10.1016/j.ijhydene.2006.12.026.

[13] MethQuest (2022): *MethQuest*. [accessed: 08-08-2025] Available at: https://www.methquest.de/fileadmin//user_upload/downloads/PMs/MethQuest_ExecutiveSummary.pdf.

[14] Heimann N, Raab M, Haas S, Pichlmaier S, Wulff N, Dietrich R-U. *Contribution to a standardized economic and ecological assessment methodology for e-fuel production in Germany*. Front Energy Res 2025.

[15] Gorre J, Ortloff F, van Leeuwen C. *Production costs for synthetic methane in 2030 and 2050 of an optimized Power-to-Gas plant with intermediate hydrogen storage*. Appl Energy 2019;253:113594. https://doi.org/10.1016/j.apenergy.2019.113594.

[16] Vega PE, Moumin G, Neumann NC, Roeb M, Ardone A, Sattler C. *Holistic view on synthetic natural gas production: a technical, economic and environmental analysis*. Energies 2022;15. https://doi.org/10.3390/en15051608.

[17] Guilera J, Ramon MJ, Andreu T. *Economic viability of SNG production from power and CO2*. Energ Conver Manage 2018;162:218–24. https://doi.org/10.1016/j.enconman.2018.02.037.

[18] Peters R, Baltruweit M, Grube T, Samsun RC, Stolten D. *A techno economic analysis of the power to gas route*. J CO2 Util 2019;34:616–34. https://doi.org/10.1016/j.jcou.2019.07.009.

[19] De Paolis R, Bernardini V, Campana LG, Ermini MV, Verna M, Raimondi G, et al. *Techno-economic and climate finance assessment of a methanation plant with green hydrogen production and CO2 recycling in Italy*. Int J Hydrogen Energy 2024. https://doi.org/10.1016/j.ijhydene.2024.07.137.

[20] Rahmat Y, Maier S, Moser F, Raab M, Hoffmann C, Repke J-U, et al. *Techno-economic and exergy analysis of e-methanol production under fixed operating conditions in Germany*. Appl Energy 2023;351. https://doi.org/10.1016/j.apenergy.2023.121738.

[21] DIN (2017): *DIN EN 16723-2*. Erdgas und Biomethan zur Verwendung im Transportwesen und Biomethan zur Einspeisung ins Erdgasnetz – Teil 2: Festlegungen für Kraftstoffe für Kraftfahrzeuge; Deutsche Fassung EN16723-2: 2017, DIN.

[22] DVGW e.V. (2013): *DVGW-Arbeitsblatt G260 (A)*.

[23] Koschany F, Schlereth D, Hinrichsen O. *On the kinetics of the methanation of carbon dioxide on coprecipitated NiAl (O) x*. Appl Catal B 2016;181:504–16.

[24] Wärtsilä (2022): *Wärtsilä Methane Number Calculator*. [accessed: 09-27-2023] Available at: https://www.wartsila.com/marine/products/gas-solutions/methane-number-calculator.

[25] RMG Messtechnik GmbH (2024): Berechnungen nach ISO 6976. [accessed: 09-06-2024] Available at: https://www.rmg.com/de/veroeffentlichungen/online-tools/berechnungen-nach-iso-6976.

[26] Becker WL, Penev M, Braun RJ. *Production of synthetic natural gas from carbon dioxide and renewably generated hydrogen: a techno-economic analysis of a power-to-gas strategy*. J Energy Res Technol 2019;141(2). https://doi.org/10.1115/1.4041381.

[27] Raab M, Körner R, Dietrich R-U. *Techno-economic assessment of renewable hydrogen production and the influence of grid participation*. Int J Hydrogen Energy 2022;47 (63):26798–811.

[28] Grave K., Hazrat M., Boeve S., von Blücher F., Bourgault C., Bader N., Breitschopf B., Friedrichsen N., Arens M., Aydemir A., Pudlik M., Duscha V., Ordonez J., Lutz C., Großmann A., Flaute M. (2015): *Stromkosten der energieintensiven Industrie: Ein internationaler Vergleich - Zusammenfassung der Ergebnisse* -. Fraunhofer ISI, ECOFY.

[29] EpexSpot (2020): *Marktintegration erneuerbarer Energien – Mission erfüllt?*.

[30] Bundesnetzagentur (2024): *Großhandelspreise* [accessed: 02-27-2025] Available at: https://www.smard.de/.

[31] Climate Data Center (2022). [accessed: 02-27-2025] Retrieved from: https://cdc.dwd.de/portal/.

[32] IRENA (2021): *Renewable Power Generation Costs in 2020*, in: Agency I.R.E., (Ed.). ISBN 978-92-9260-348-9.

[33] Klose J. *Kinetics of the methanation of carbon monoxide on an alumina-supported nickel catalyst*. J Catal 1984;85(1):105–16. https://doi.org/10.1016/0021-9517(84)90114-3.

[34] Harms H, Höhlein B, Skov A. *Methanisierung kohlenmonoxidreicher gase beim energietransport*. Chem Ing Tech 1980;52(6):504–15. https://doi.org/10.1002/cite.330520605.

[35] Zhang J, Fatah N, Capela S, Kara Y, Guerrini O, Khodakov AY. *Kinetic investigation of carbon monoxide hydrogenation under realistic conditions of methanation of biomass derived syngas*. Fuel 2013;111:845–54. https://doi.org/10.1016/j.fuel.2013.04.057.

[36] Rönsch S, Köchermann J, Schneider J, Matthischke S. *Global reaction kinetics of CO and CoO_2 methanation for dynamic process modeling*. Chem Eng Technol 2016;39(2): 208–18. https://doi.org/10.1002/ceat.201500327.

[37] Elnashaie S.S.E.H., Elshishini S.S. (1993): *Modelling, simulation and optimization of industrial fixed bed catalytic reactors. Topics in chemical engineering, Volume 7*. United States. New York, NY (United States); Gordon and Breach Science Publishers, Inc.

[38] Koschany F. *Experimentelle studien zur methanisierung von CO_2 auf nickelkatalysatoren*. Technische Universität München; 2016.

[39] Aparicio LM. *Transient isotopic studies and microkinetic modeling of methane reforming over nickel catalysts*. J Catal 1997;165(2):262–74. https://doi.org/10.1006/jcat.1997.1468.

[40] Energiesystem-Forschung (2021): *Projekt BEniVer Begleitforschung zur „Energiewende im Verkehr“*. [accessed: 12-08-2021]. Available at: https://www.energiesystem-forschung.de/forschen/projekte/beniver-begleitforschung.

[41] Champon I, Bengaouer A, Chaise A, Thomas S, Roger A-C. *Carbon dioxide methanation kinetic model on a commercial Ni/Al2O3 catalyst*. J CO2 Util 2019;34: 256–65. https://doi.org/10.1016/j.jcou.2019.05.030.

[42] Haldor Topsøe (2011): *From coal to clean energy*. [accessed: 08-29-2025] Available at: https://www.netl.doe.gov/sites/default/files/netl-file/from-coal-to-clean-energy-march-april-2011.pdf.

[43] Yuan XZ, He CY, Namkung H, Fan SM, Kim H-T. *Process modeling and performance evaluation of commercial-scale coal-to-SNG plant using Indonesia IBC coal with two drying concepts*. Asia Pac J Chem Eng 2016;11(6):1012–26. https://doi.org/10.1002/apj.2036.

[44] Haldor Topsøe (2009): *From solid fuels to substitute natural gas (SNG) using TREMP™*. [accessed: 08-04-2025] Available at: https://www.netl.doe.gov/sites/default/files/netl-file/tremp-2009.pdf.

[45] Meylan FD, Moreau V, Erkman S. *Material constraints related to storage of future European renewable electricity surpluses with CO2 methanation*. Energy Policy 2016; 94:366–76. https://doi.org/10.1016/j.enpol.2016.04.012.

[46] Peters M, Timmerhaus K, West R. *Plant design and economics for chemical engineers*. ISBN: New York McGraw-Hill; 2004.

[47] Albrecht FG, König DH, Baucks N, Dietrich R-U. *A standardized methodology for the techno-economic evaluation of alternative fuels – a case study*. Fuel 2017;194:511–26. https://doi.org/10.1016/j.fuel.2016.12.003.

[48] Maier S, Tuomi S, Kihlman J, Kurkela E, Dietrich R-U. *Techno-economically-driven identification of ideal plant configurations for a new biomass-to-liquid process – a case study for Central-Europe*. Energ Conver Manage 2021;247:114651. https://doi.org/10.1016/j.enconman.2021.114651.

[49] Chemical Engineering. Chemical Engineering Plant Cost Index. [accessed: 07-25-2025] Available at: https://www.chemengonline.com/pci-home.

[50] Hannula I. *Hydrogen enhancement potential of synthetic biofuels manufacture in the European context: a techno-economic assessment*. Energy 2016;104:199–212.

[51] Hamelinck CN, Faaij AP. *Outlook for advanced biofuels*. Energy Policy 2006;34(17): 3268–83.

[52] Woods DR. *Rules of thumb in engineering practice*. ISBN 3527611126: John Wiley & Sons; 2007.

[53] Eurostat (2025): *Gas prices for non-household consumers - bi-annual data (from 2007 onwards)*. [accessed: 08-01-2025] Available at: https://ec.europa.eu/eurostat/databrowser/view/nrg_pc_203_custom_17644735/default/table.

[54] Methanex (2025): *Methanex Monthly Average Regional Posted Contract Price History*. [accessed: 08-01-2025] Available at: https://www.methanex.com/our-products/about-methanol/pricing/.

[55] Statista (2022): *Industrial natural gas prices in the European Union from 2008 to 2020, by consumption*. [accessed: 09-26-2023] Available at: https://www.statista.com/statistics/1047070/natural-gas-price-european-union/.

[56] Spinelli E.B., Tobias; Franca, Lucas (2025): *Renewable gases in Europe: from fossil fuels to H2 and biomethane*, in *online session*, ata insights. [accessed: 01-30-2025] Retrieved from: https://www.youtube.com/watch?v=ZnzkThgwD8M.

[57] DVGW e.V. (2025): *H2 in der Fläche –Gasverteilnetze für Kraftwerke und Wirtschaftsstandorte*. DVGW Wissenswert.

[58] European Court of Auditors (2024): *Renewable hydrogen-powered EU: auditors call for a reality check*.

[59] European Union Agency for the Cooperation of Energy Regulators (2023): *Gas Fact sheet*. [accessed: 02-26-2025] Available at: https://www.acer.europa.eu/gas-factsheet.

[60] Gas Infrastructure Europe (2023): Storage Database. [accessed: 02-26-2025] Available at: https://www.gie.eu/transparency/databases/storage-database/.

[61] DVGW e.V. (2025): *Roadmap Gas 2050*. [accessed: 01-22-2025] Available at: https://www.dvgw.de/themen/forschung-und-innovation/energieforschung/roadmap-gas-2050.

[62] Bartsch V.K., Florian; Grönner, Jürgen (2024): *Gasnetzgebietstransformationsplan*, in *Wasserstoff über die Gasverteilnetze für alle nutzbar machen*. [accessed: 04-25-2025] Available at: https://www.h2vorort.de/fileadmin/Redaktion/PDF/gtp-2024-Leitfaden_1.1.pdf.

[63] DVGW e.V. (2024): *DVGW-Arbeitsblatt G685*. [accessed: 02-27-2025] Available at: https://shop.wvgw.de/G-685-8-Arbeitsblatt-11-2024/512416.

[64] Bundesamt für Justitz (2005): *Gesetz über die Elektrizitäts- und Gasversorgung (Energiewirtschaftsgesetz - EnWG)*. [accessed: 05-30-2025] Available at: https://www.gesetze-im-internet.de/enwg_2005/BJNR197010005.html.

[65] Bundesnetzagentur (2025): *Energiemarkt aktuell. Der Gasmarkt im Jahr 2024*. [accessed: 02-27-2025] Available at: https://www.smard.de/page/home/topic-article/211784/215644.

[66] Deutscher Bundestag (2024): *Europäischer Binnen-/Wasserstoffmarkt Mittwoch, 5. Juni 2024 Öffentlichen Sitzung des Parlamentarischen Beirates für nachhaltige Entwicklung.*.

[67] Schaffert D.J.H., Lukas; Brede, Nils; Grube, Elisabeth; Pietsch, Philipp; Mörs, Friedemann; Staudt, Christiane (2024): *Vielversprechende Zukunftsoptionen für Biogas: Ergebnisse des DVGW-Forschungsprojektes „ENEVEG“*. Available at: https://www.dvgw-ebi.de/medien/dvgw-ebi/2_themen/publikationen/2024-jan-staudt-ewp.pdf.

[68] Destatis (2027): *Benzin im Jahr 2023 in Höhe von 15,0 Milliarden Euro versteuert*. [accessed: 02-27-2025] Available at: https://www.destatis.de/DE/Themen/Staat/Steuern/Verbrauchsteuern/energiesteuer.html.
[69] ADAC e.V. (2024): *Benzinpreis und Dieselpreis: So entstehen die Spritpreise aktuell*. [accessed: 02-27-2025] Available at: https://www.adac.de/verkehr/tanken-kraftstoff-antrieb/tipps-zum-tanken/7-fragen-zum-benzinpreis/.
[70] ADAC e.V. (2024): *Immer weniger CNG an Tankstellen: Ein Problem für Erdgasauto-Besitzer?* [accessed: 02-27-2025] Available at: https://www.adac.de/verkehr/tanken-kraftstoff-antrieb/alternative-antriebe/cng-tankstellen/.
[71] energiesystem-forschung (2022): *Projekt CombiFuel -Übergangslösung zur Wasserstoffmobilität für Verbrenner-*. [accessed: 10-25-2024] Available at: https://www.energiesystem-forschung.de/forschen/projekte/combifuel.
[72] Graforce GmbH (2024): *H2/natural gas refuelling*. [accessed: 03-10-2025] Available at: https://www.graforce.com/en/products/h2-natural-gas-refuelling.
[73] Hydrogen Council (2025): *Topsoes neue SOEC-Fabrik: Pionierprojekt zur Wasserstoffproduktion geht online*. [accessed: 03-12-2025] Available at: https://hydrogencouncil.com/de/topsoes-new-soec-factory-a-pioneering-effort-at-hydrogen-production-comes-online/.